

TMD's at High Density: Quasi-Classical Approximation

Part 1 of 2

Matthew D. Sievert

with Yuri Kovchegov

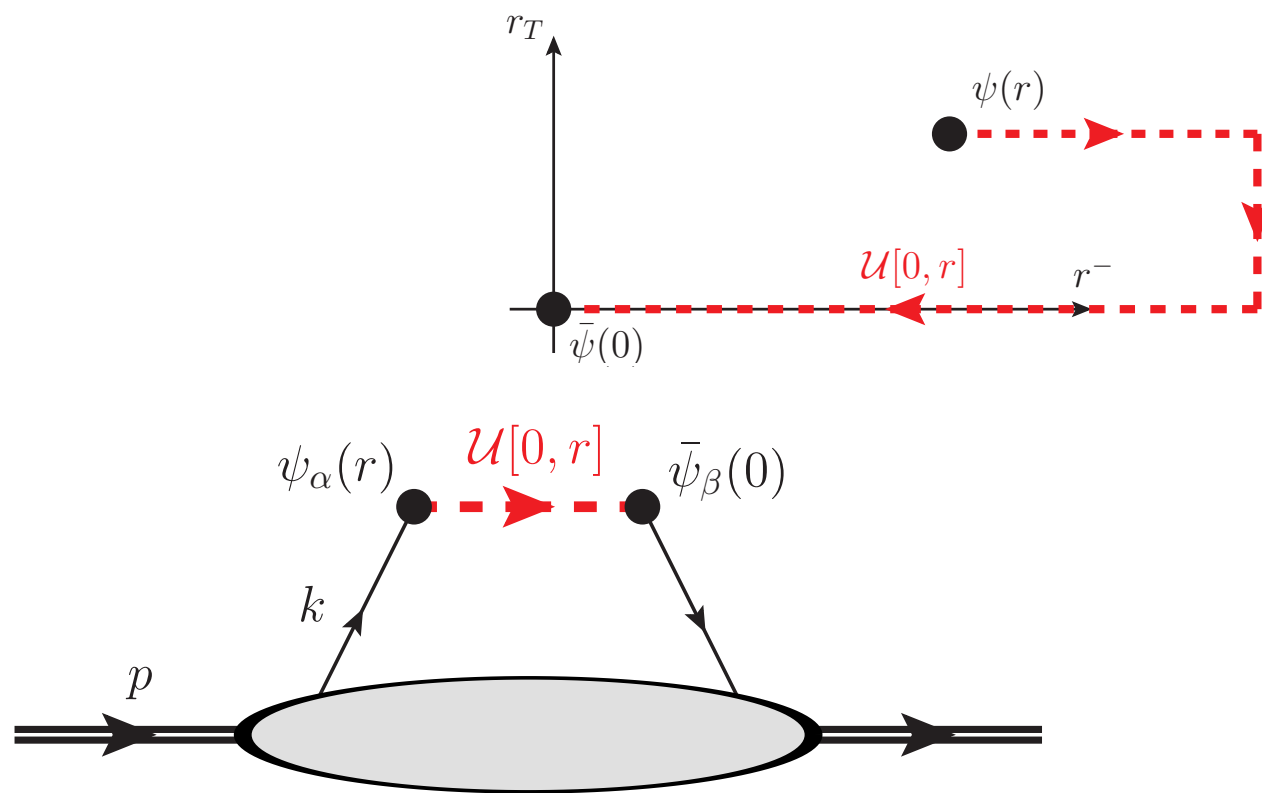


1505 .01176
1310 .5028

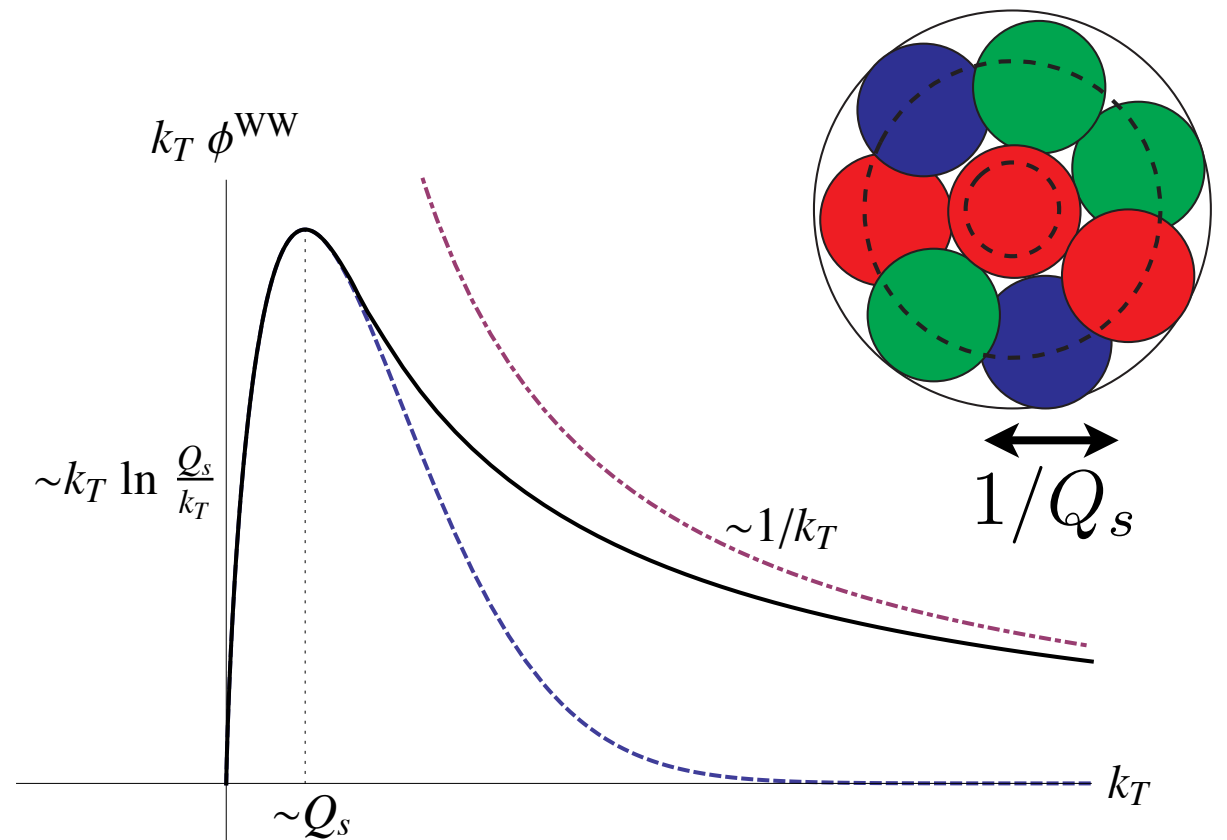
EIC Users' Group Meeting
Friday Jan. 8, 2016

Overview

TMD's: Quark Spin / Orbit Distributions



High-Density Gluon Fields: Intrinsic Hard Scale Q_s



- Hard scale Q_s leads to factorization of the TMD's themselves.
- Calculable structure from first-principles QCD

Quark Anatomy of a Spin-1/2 Hadron

$$\phi_{\alpha\beta}(x, \vec{k}_{\perp}) = \int \frac{d^2-r}{(2\pi)^3} e^{ik \cdot r} \langle h(p, S) | \bar{\psi}_{\beta}(0) \mathcal{U}[0, r] \psi_{\alpha}(r) | h(p, S) \rangle$$

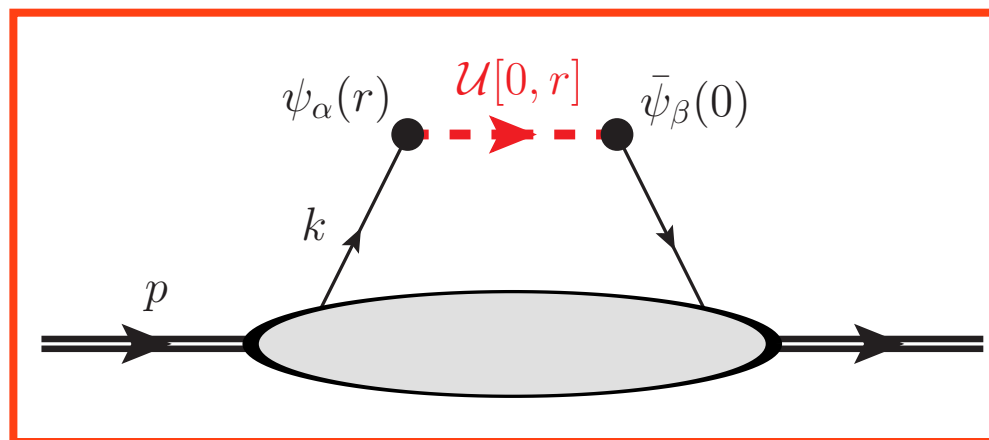
Quark Anatomy of a Spin-1/2 Hadron

$$\phi_{\alpha\beta}(x, \vec{k}_{\perp}) = \int \frac{d^2-r}{(2\pi)^3} e^{ik \cdot r} \langle h(p, S) | \bar{\psi}_{\beta}(0) \mathcal{U}[0, r] \psi_{\alpha}(r) | h(p, S) \rangle$$

		Quark Polarization		
		Un-Polarized (U)	Longitudinally Polarized (L)	Transversely Polarized (T)
Nucleon Polarization	U	$f_1 = \odot$		$h_1^{\perp} = \odot - \odot$ Boer-Mulders
	L		$g_{1L} = \odot \rightarrow - \odot \rightarrow$ Helicity	$h_{1L}^{\perp} = \odot \rightarrow - \odot \rightarrow$
	T	$f_{1T}^{\perp} = \odot \uparrow - \odot \downarrow$ Sivers	$g_{1T}^{\perp} = \odot \uparrow - \odot \uparrow$	$h_1 = \odot \uparrow - \odot \uparrow$ Transversity $h_{1T}^{\perp} = \odot \rightarrow - \odot \rightarrow$
Γ		γ^+	$\gamma^+ \gamma^5$	$\gamma^+ \gamma_{\perp}^i \gamma^5$

- **3D distributions** of quarks with spin and momentum.

Quark Anatomy of a Spin-1/2 Hadron

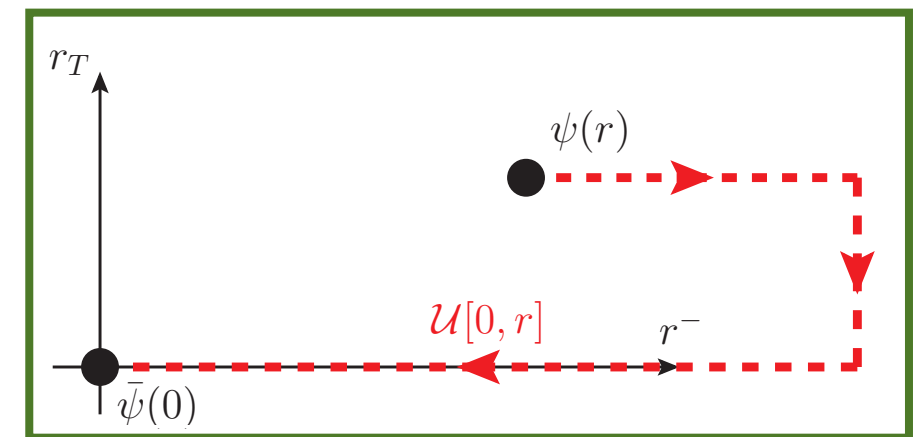
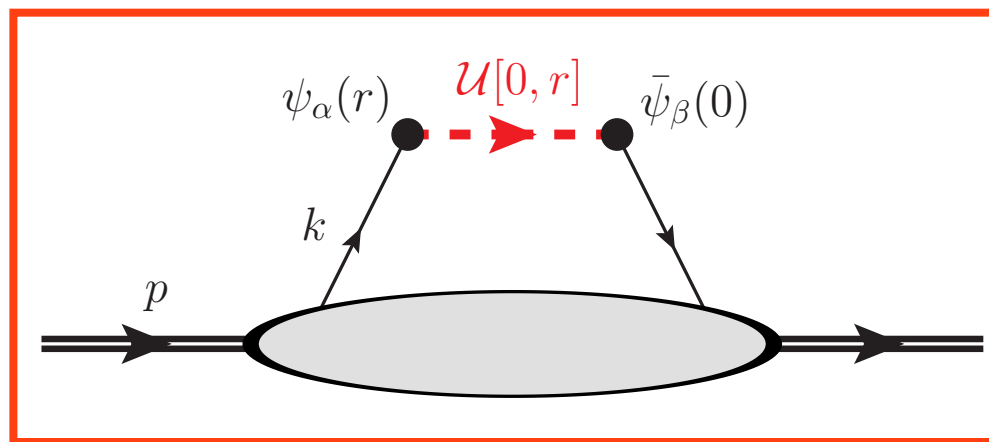


$$\phi_{\alpha\beta}(x, \vec{k}_\perp) = \int \frac{d^2-r}{(2\pi)^3} e^{ik \cdot r} \langle h(p, S) | \bar{\psi}_\beta(0) \mathcal{U}[0, r] \psi_\alpha(r) | h(p, S) \rangle$$

		Quark Polarization		
		Un-Polarized (U)	Longitudinally Polarized (L)	Transversely Polarized (T)
Nucleon Polarization	U	$f_1 = \odot$		$h_1^\perp = \odot - \odot$ Boer-Mulders
	L		$g_{1L} = \odot \rightarrow - \odot \rightarrow$ Helicity	$h_{1L}^\perp = \odot \rightarrow - \odot \rightarrow$
	T	$f_{1T}^\perp = \odot \uparrow - \odot \downarrow$ Sivers	$g_{1T}^\perp = \odot \uparrow - \odot \uparrow$	$h_1 = \odot \uparrow - \odot \uparrow$ Transversity $h_{1T}^\perp = \odot \uparrow - \odot \uparrow$
Γ		γ^+	$\gamma^+ \gamma^5$	$\gamma^+ \gamma_\perp^i \gamma^5$

- **3D distributions** of quarks with spin and momentum.
- **Bilocal quark fields**, connected by a staple-shaped **gauge link**.

Quark Anatomy of a Spin-1/2 Hadron



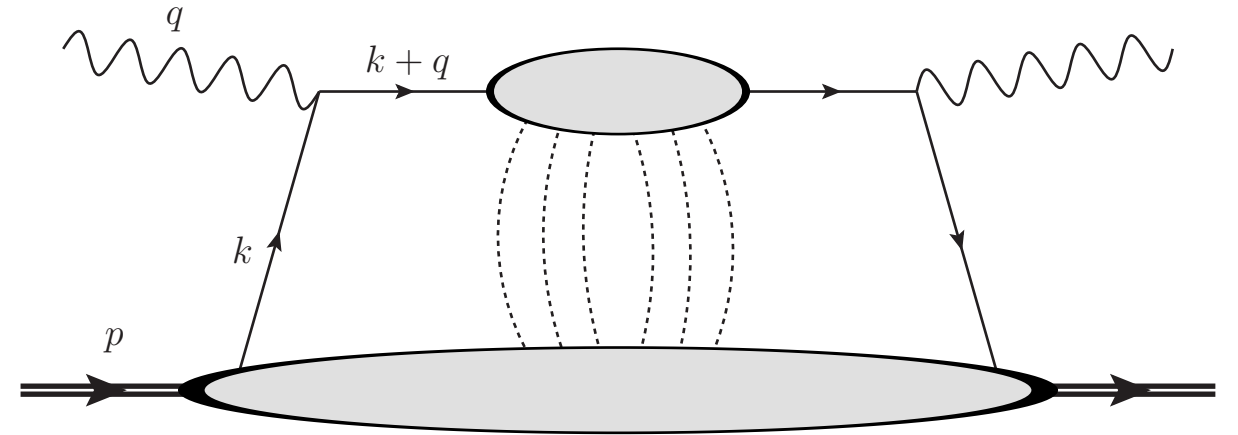
$$\phi_{\alpha\beta}(x, \vec{k}_\perp) = \int \frac{d^2-r}{(2\pi)^3} e^{ik \cdot r} \langle h(p, S) | \bar{\psi}_\beta(0) \mathcal{U}[0, r] \psi_\alpha(r) | h(p, S) \rangle$$

		Quark Polarization		
		Un-Polarized (U)	Longitudinally Polarized (L)	Transversely Polarized (T)
Nucleon Polarization	U	$f_1 = \odot$		$h_1^\perp = \odot - \odot$ Boer-Mulders
	L		$g_{1L} = \odot \rightarrow - \odot \rightarrow$ Helicity	$h_{1L}^\perp = \odot \rightarrow - \odot \rightarrow$
	T	$f_{1T}^\perp = \odot \uparrow - \odot \downarrow$ Sivers	$g_{1T}^\perp = \odot \uparrow - \odot \uparrow$	$h_1 = \odot \uparrow - \odot \uparrow$ Transversity $h_{1T}^\perp = \odot \uparrow - \odot \uparrow$
Γ		γ^+	$\gamma^+ \gamma^5$	$\gamma^+ \gamma_\perp^i \gamma^5$

- **3D distributions** of quarks with spin and momentum.
- **Bilocal quark fields**, connected by a staple-shaped **gauge link**.
- Gauge fields describe **physical distortion** of quark momentum.

Gauge Fields: Dilute vs. Dense Systems

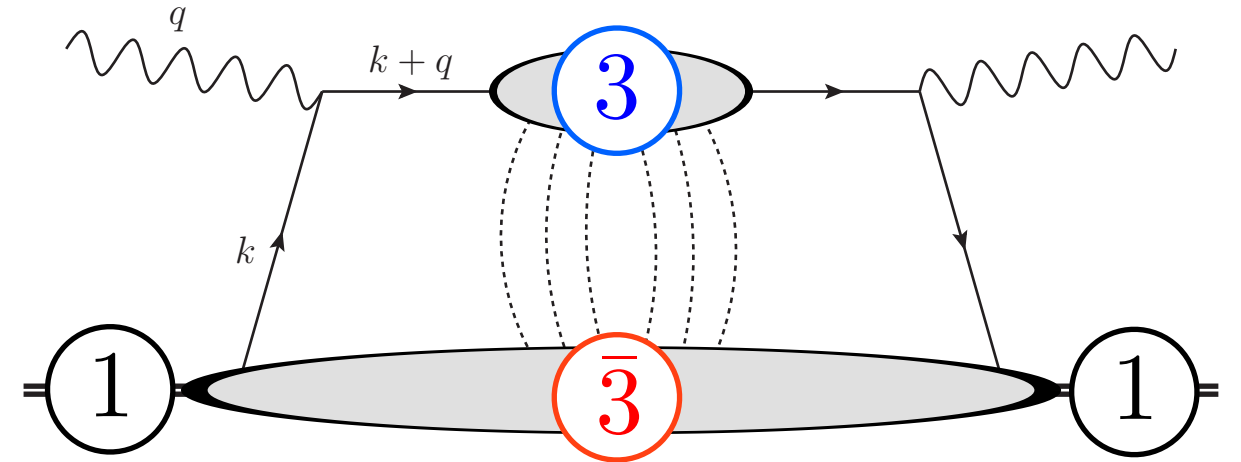
Dilute Systems: Lensing



Gauge Fields: Dilute vs. Dense Systems

Dilute Systems: Lensing

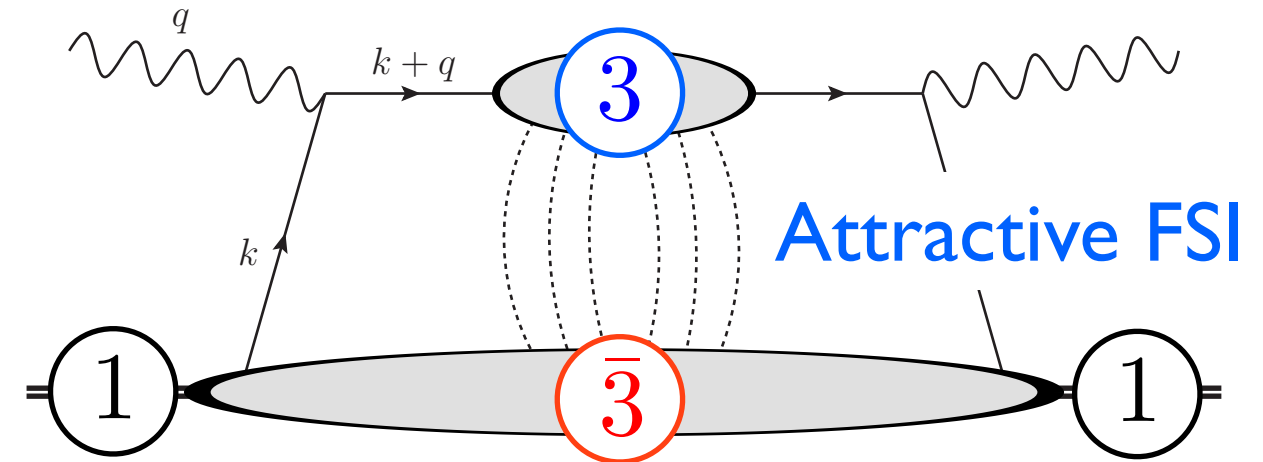
- Produced quark and hadron remnants are **color-correlated**.



Gauge Fields: Dilute vs. Dense Systems

Dilute Systems: Lensing

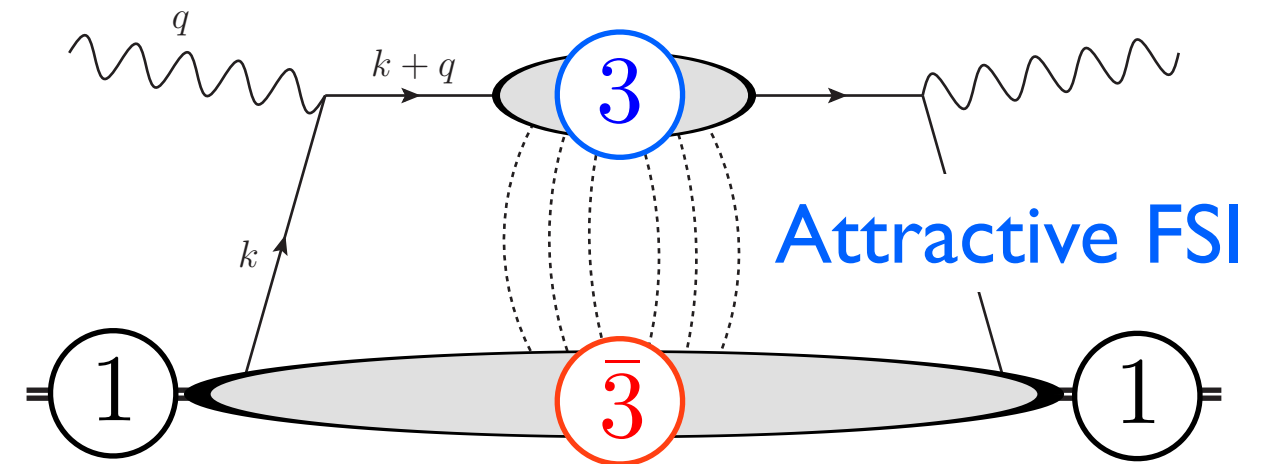
- Produced quark and hadron remnants are **color-correlated**.
- FSI are **attractive**, deflecting the observed quark **toward** remnants.



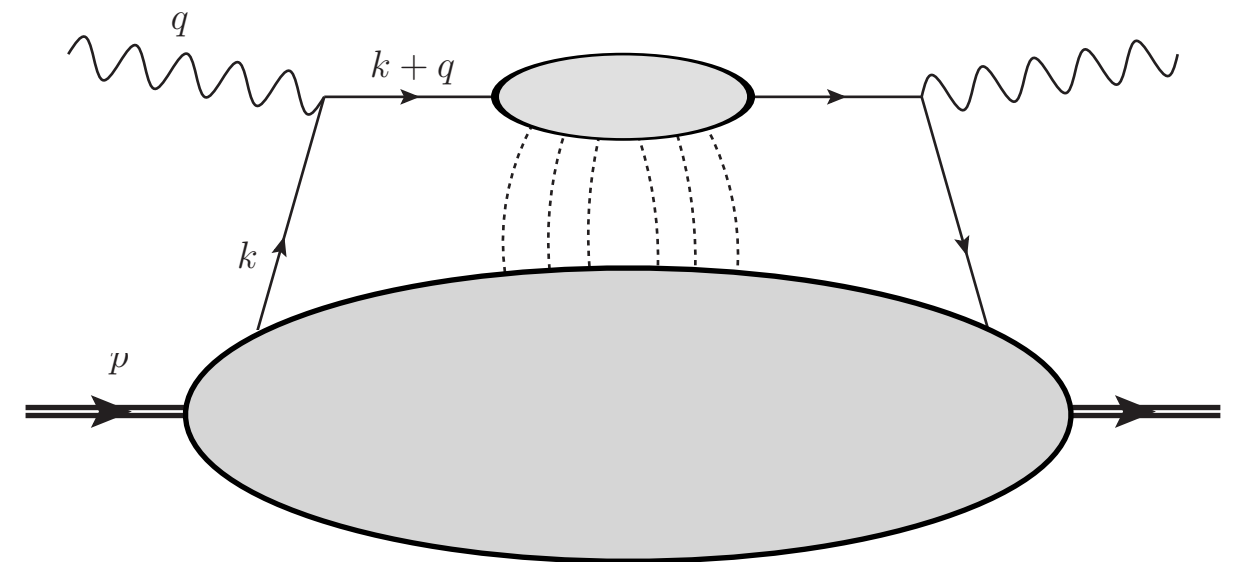
Gauge Fields: Dilute vs. Dense Systems

Dilute Systems: Lensing

- Produced quark and hadron remnants are **color-correlated**.
- FSI are **attractive**, deflecting the observed quark **toward** remnants.



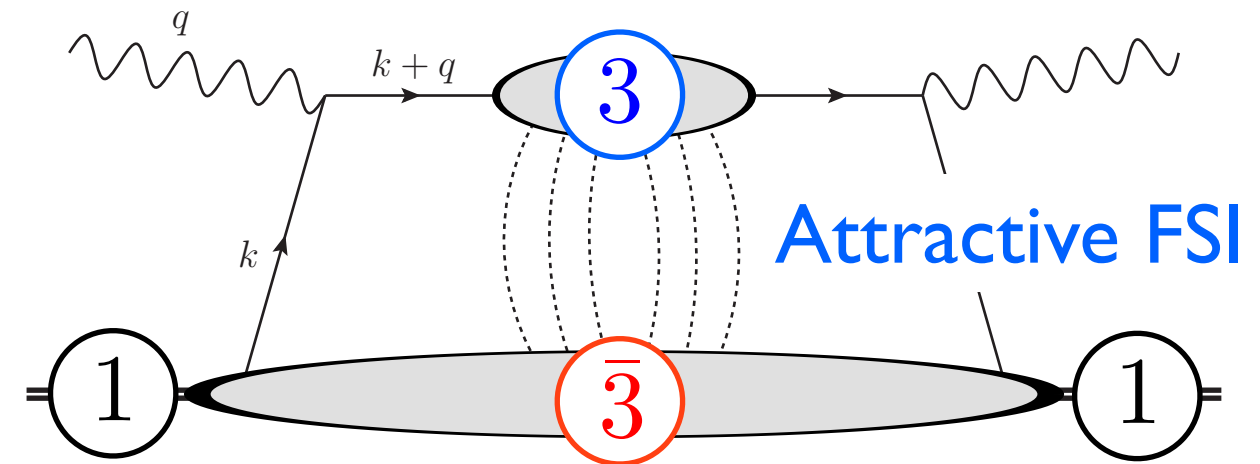
Dense Systems: Broadening



Gauge Fields: Dilute vs. Dense Systems

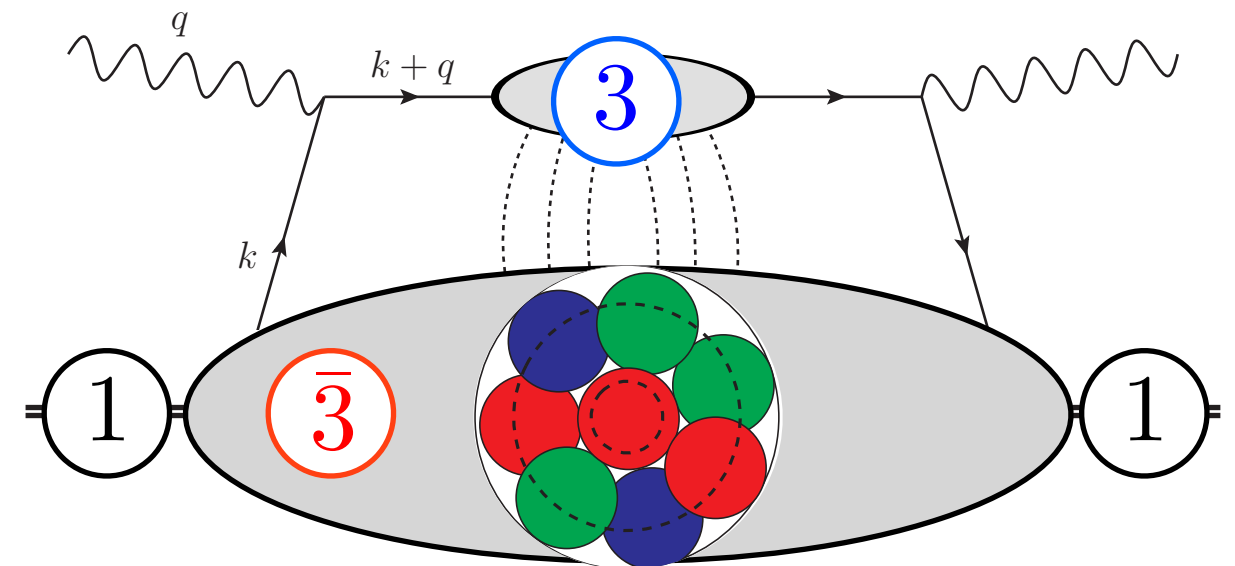
Dilute Systems: Lensing

- Produced quark and hadron remnants are **color-correlated**.
- FSI are **attractive**, deflecting the observed quark **toward** remnants.



Dense Systems: Broadening

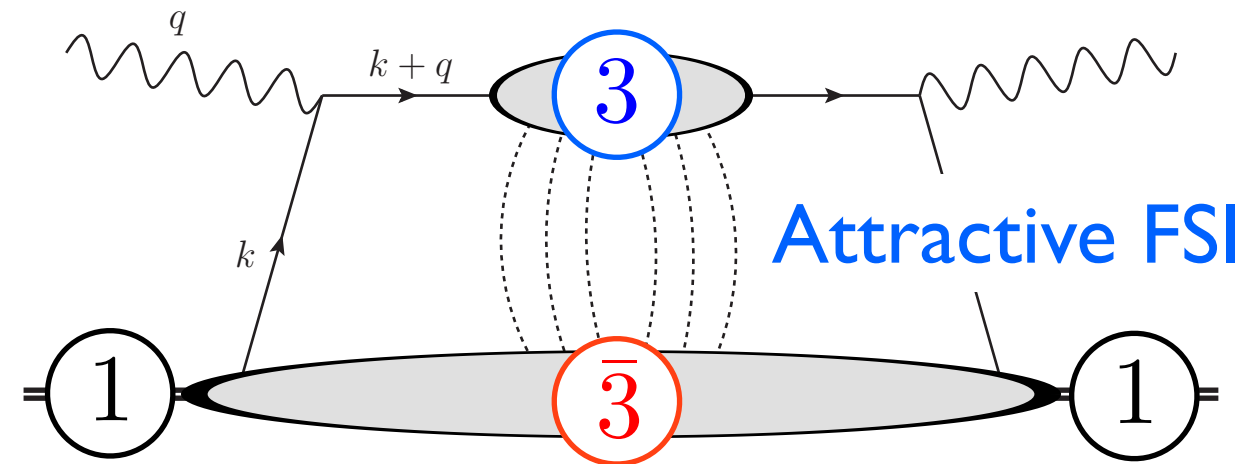
- High density **screens** the net charge.



Gauge Fields: Dilute vs. Dense Systems

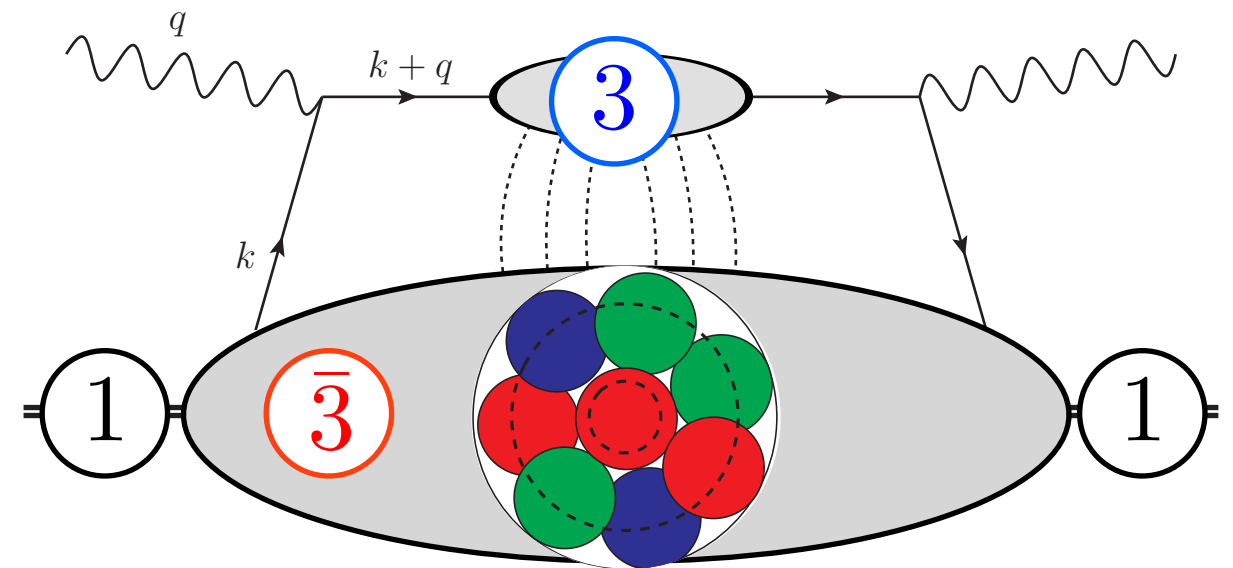
Dilute Systems: Lensing

- Produced quark and hadron remnants are **color-correlated**.
- FSI are **attractive**, deflecting the observed quark **toward** remnants.



Dense Systems: Broadening

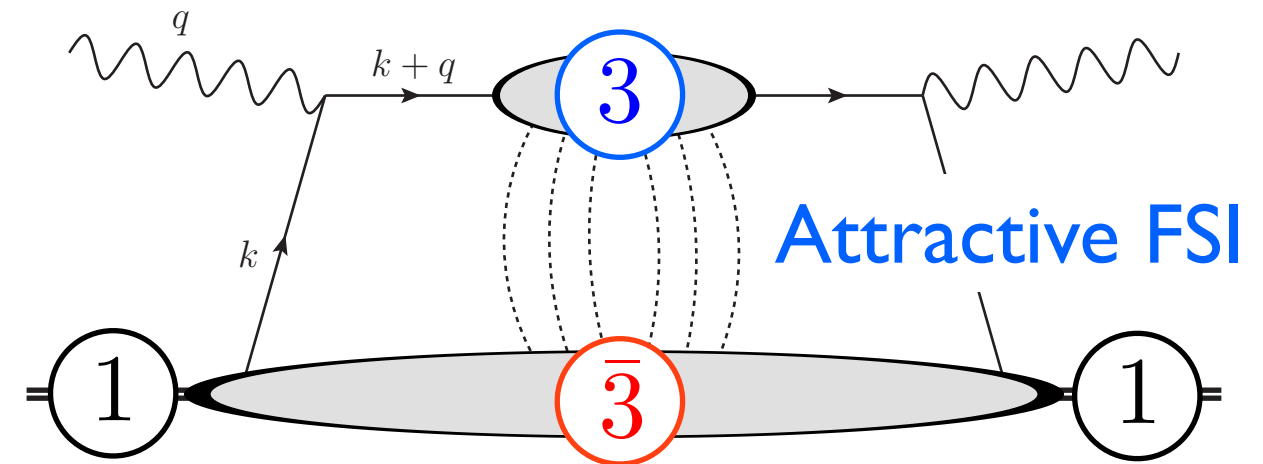
- High density **screens** the net charge.
- Rescattering occurs on the random **local charge density**.



Gauge Fields: Dilute vs. Dense Systems

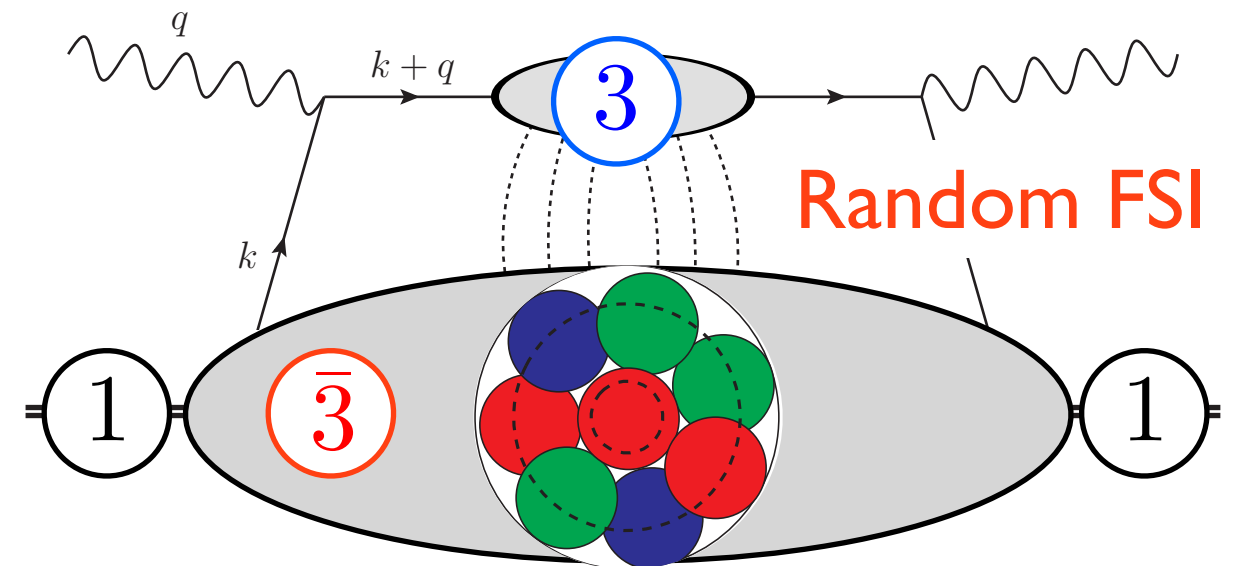
Dilute Systems: Lensing

- Produced quark and hadron remnants are **color-correlated**.
- FSI are **attractive**, deflecting the observed quark **toward** remnants.



Dense Systems: Broadening

- High density **screens** the net charge.
- Rescattering occurs on the random **local charge density**.
- FSI are **random**, broadening the quark momentum **isotropically**.

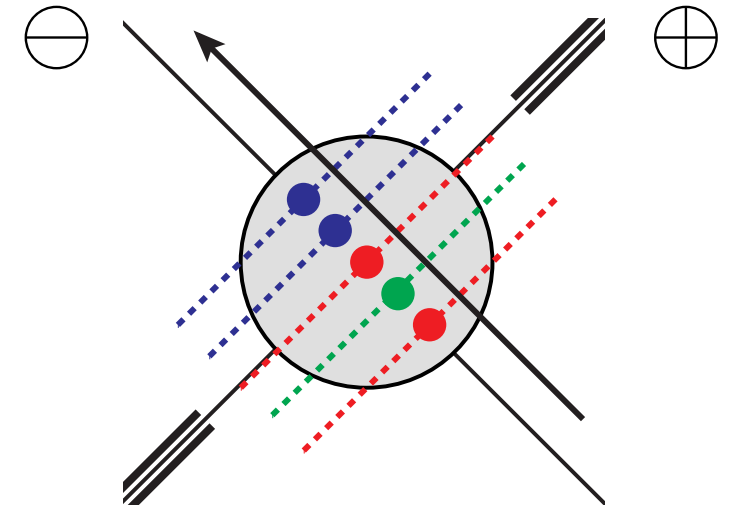


High Density: The Quasi-Classical Limit

- At high density and weak coupling, **multiple independent scattering** occurs on the **local charge density**.

Nucleus: $A \gg 1$

Proton: $\rho \gg 1$



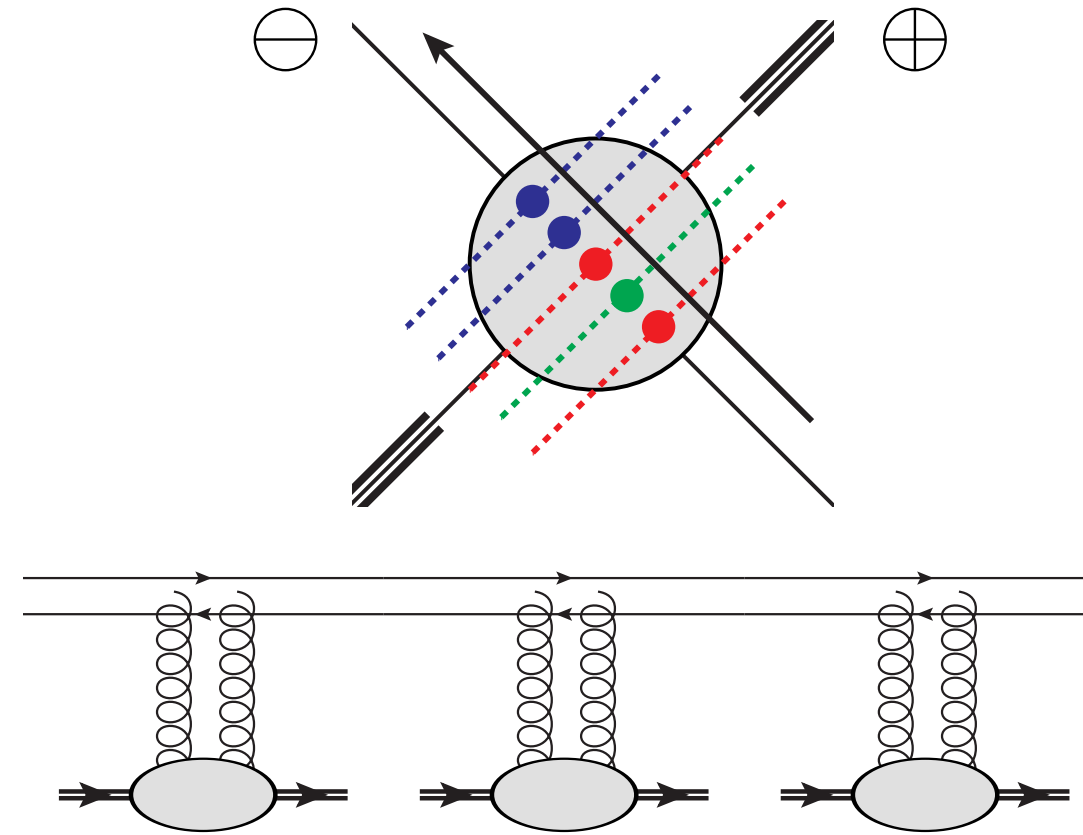
High Density: The Quasi-Classical Limit

- At high density and weak coupling, **multiple independent scattering** occurs on the **local charge density**.

Nucleus: $A \gg 1$ Proton: $\rho \gg 1$

- Resumming** the high-density effects leads to scattering in a **classical background field**.

Nucleus: $\alpha_s^2 A^{1/3} \sim 1$ Proton: $\alpha_s \rho \sim 1$



High Density: The Quasi-Classical Limit

- At high density and weak coupling, **multiple independent scattering** occurs on the **local charge density**.

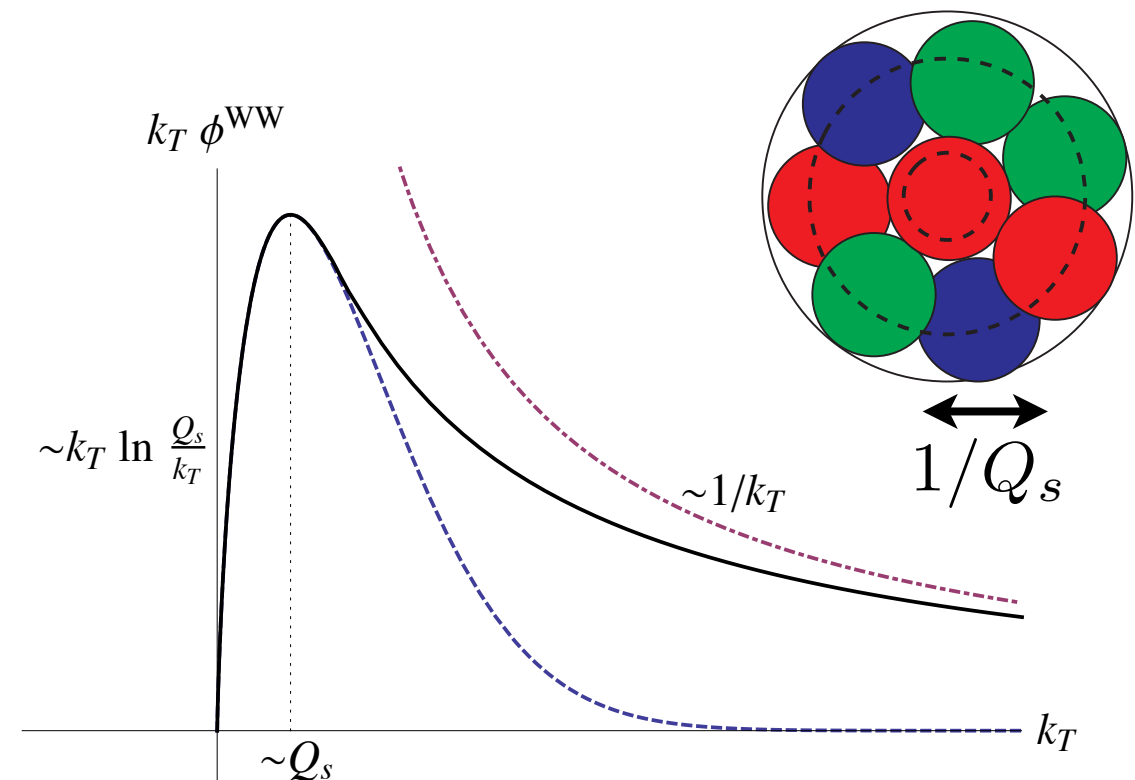
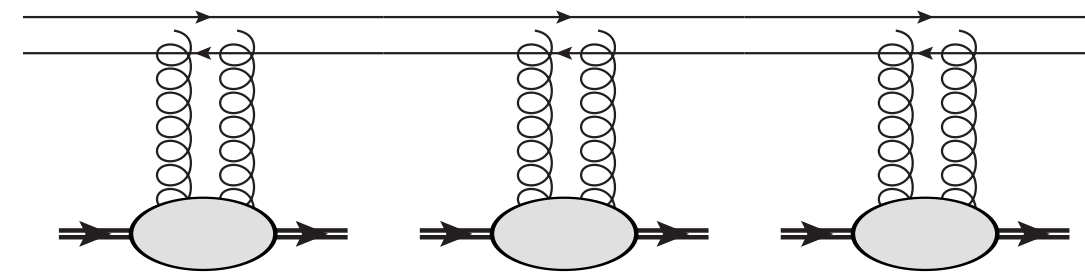
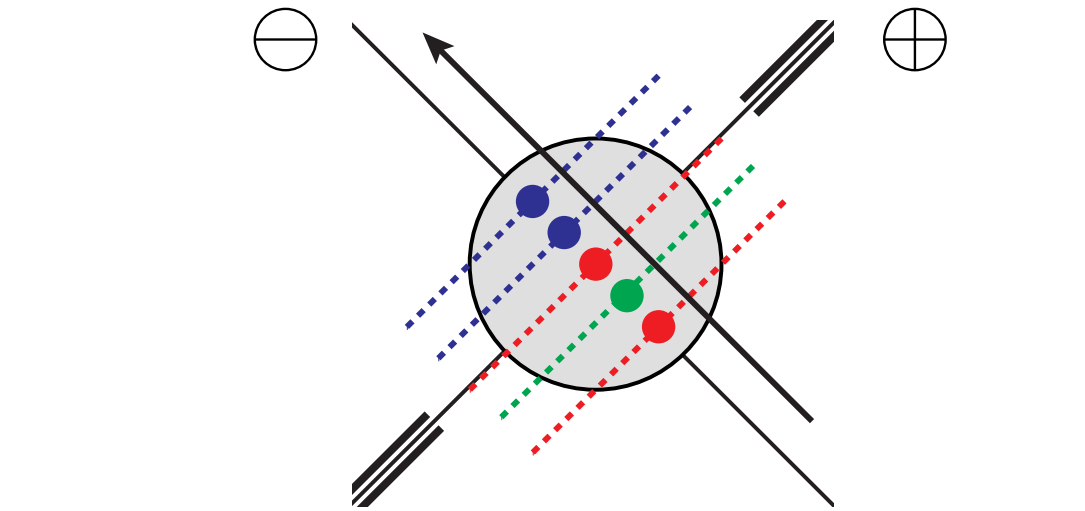
$$\text{Nucleus: } A \gg 1 \quad \text{Proton: } \rho \gg 1$$

- Resumming** the high-density effects leads to scattering in a **classical background field**.

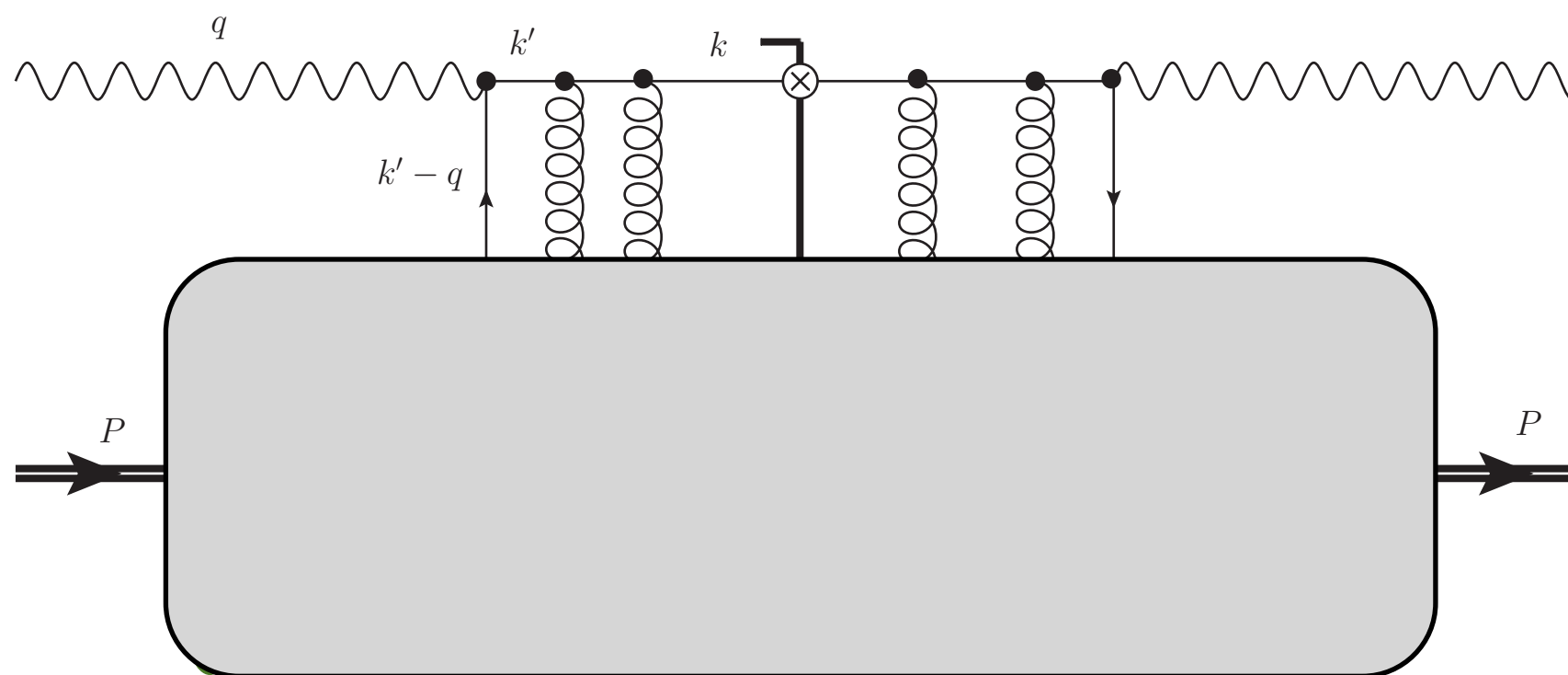
$$\text{Nucleus: } \alpha_s^2 A^{1/3} \sim 1 \quad \text{Proton: } \alpha_s \rho \sim 1$$

- High charge density defines a **hard momentum scale** Q_s which dynamically **screens the IR** gluon field.

$$\begin{aligned} \text{Both: } Q_s^2 &\propto \alpha_s^2 A^{1/3} \propto \alpha_s \rho \\ Q_s^2 &\gg \Lambda^2 \end{aligned}$$

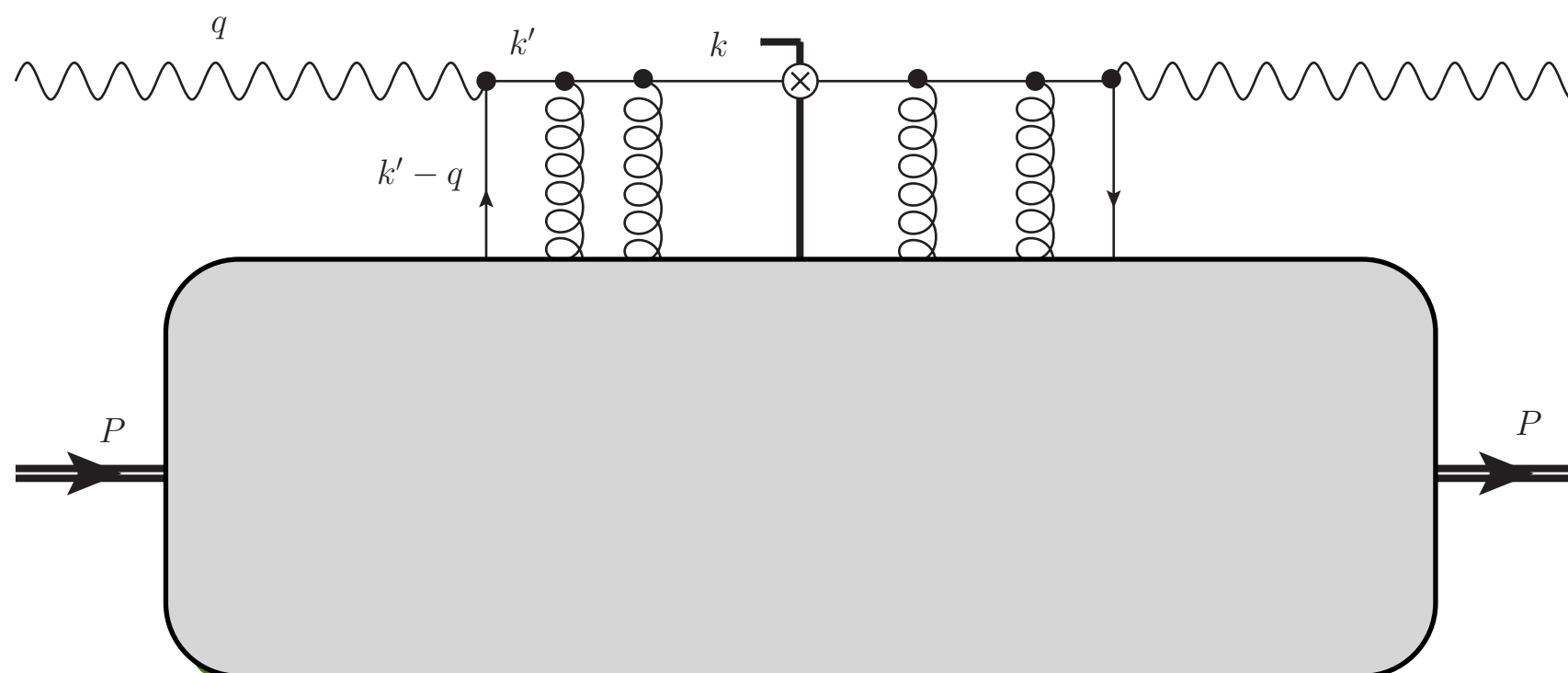


TMD's in the High-Density Limit



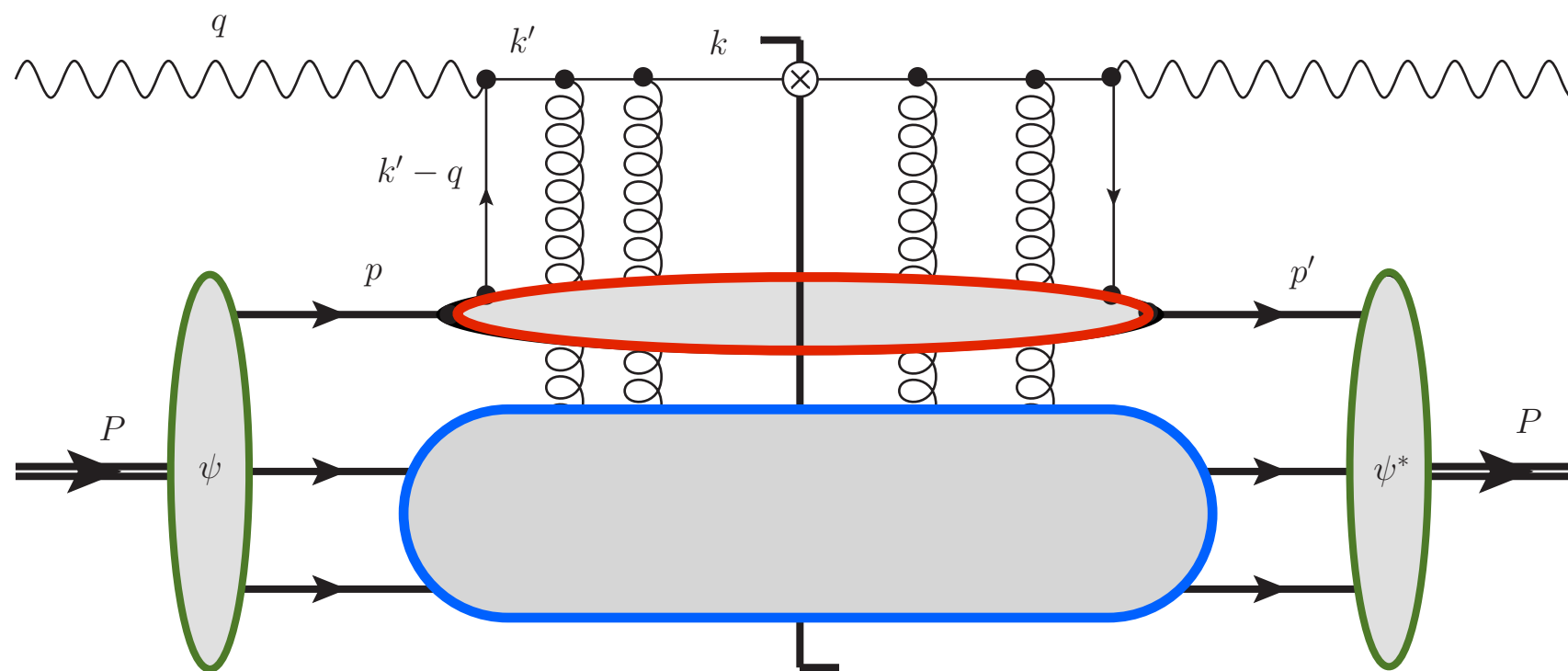
$$\langle h(p, S) | \bar{\psi}(0) \mathcal{U}[0, r] \psi(r) | h(p, S) \rangle$$

TMD's in the High-Density Limit



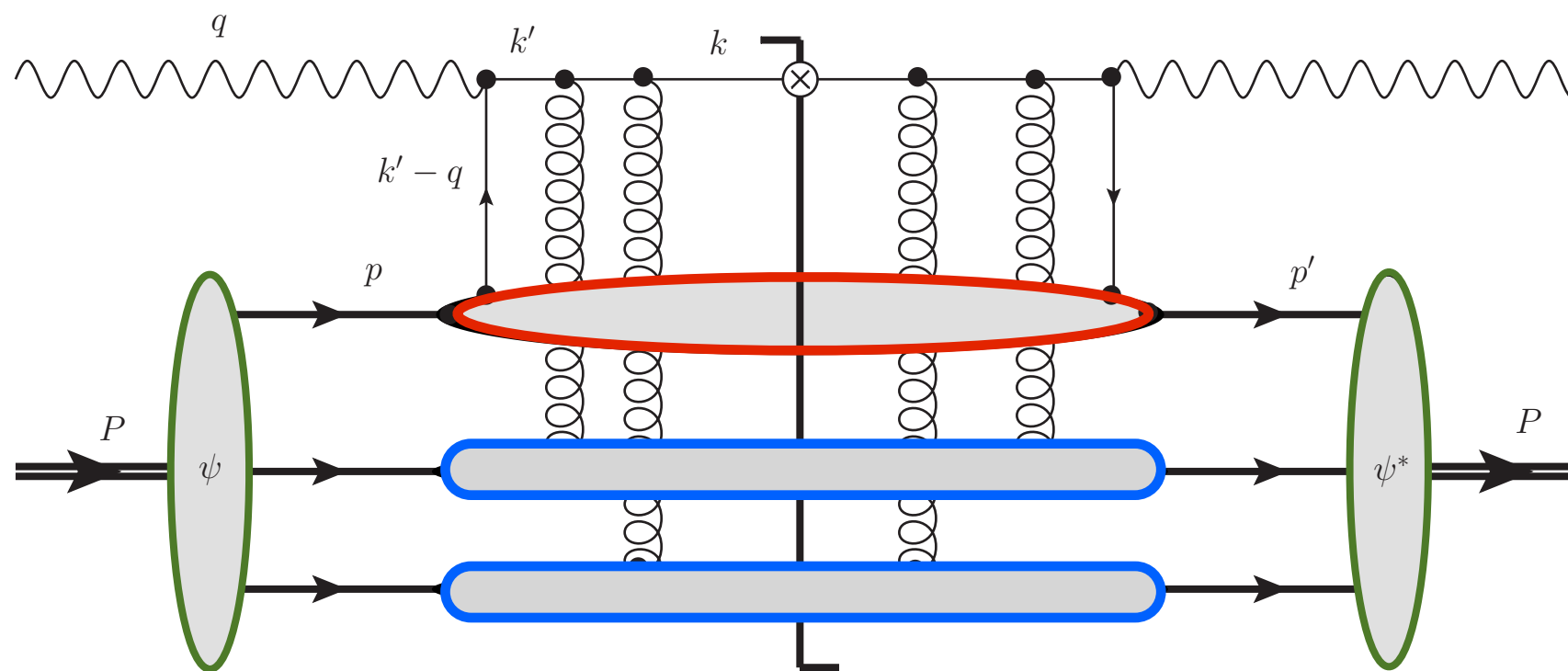
$$\langle A(p, S; Q_s) | \bar{\psi}(0) \mathcal{U}[0, r] \psi(r) | A(p, S; Q_s) \rangle$$

TMD's in the High-Density Limit



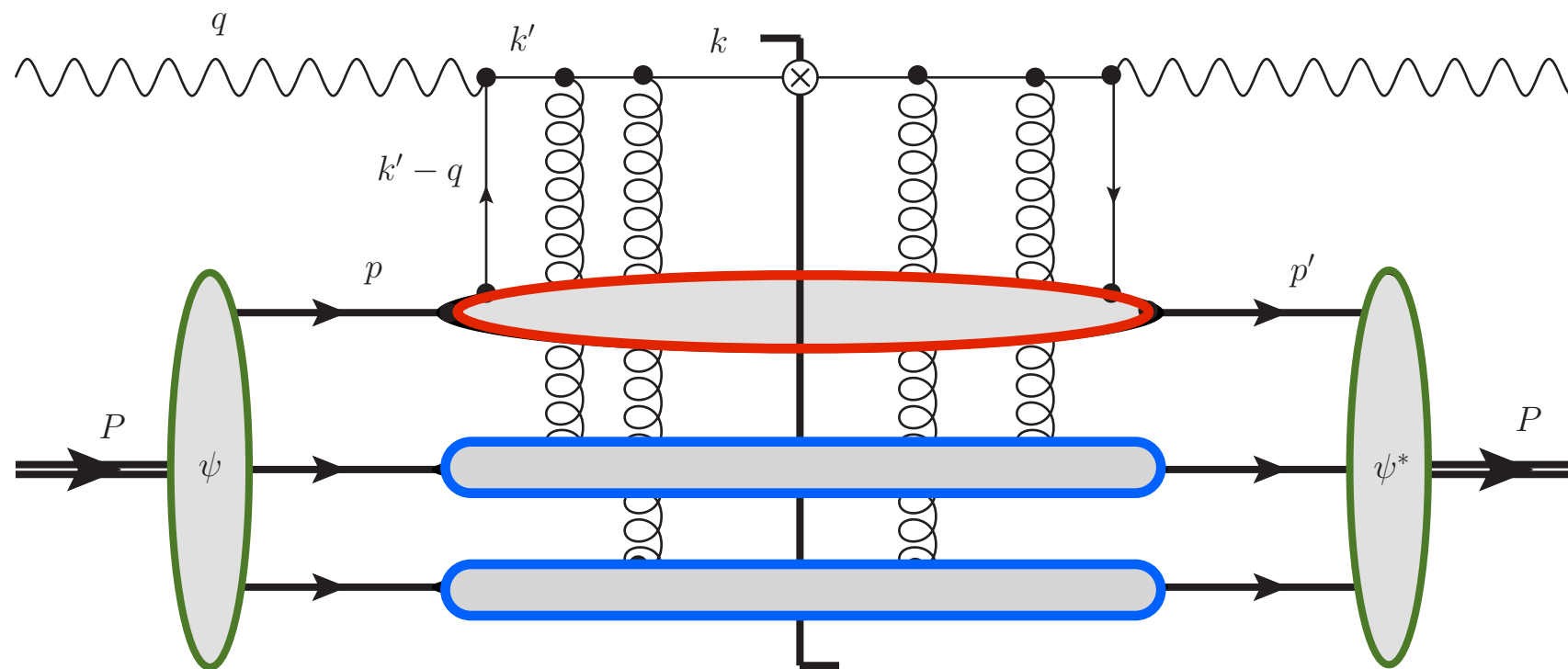
$$\left[\Psi_N^* \langle N | \bar{\psi}(0) \right] \langle (A-1) | \mathcal{U}[0, r] | (A-1) \rangle \left[\underbrace{\psi(r) | N \rangle \Psi_N}_{\text{Leading order in } A^{1/3}} \right]$$

TMD's in the High-Density Limit



$$\left[\Psi_N^* \langle N | \bar{\psi}(0) \right] \underbrace{\langle (A-1) | \mathcal{U}[0, r] | (A-1) \rangle}_{\alpha_s^2 A^{1/3} \sim \mathcal{O}(1)} \underbrace{\left[\psi(r) | N \rangle \Psi_N \right]}_{\text{Leading order in } A^{1/3}}$$

TMD's in the High-Density Limit



$$\left[\Psi_N^* \langle N | \bar{\psi}(0) \right] \underbrace{\langle (A-1) | \mathcal{U}[0, r] | (A-1) \rangle}_{\alpha_s^2 A^{1/3} \sim \mathcal{O}(1)} \underbrace{\left[\psi(r) | N \rangle \Psi_N \right]}_{\text{Leading order in } A^{1/3}}$$

$$\phi \sim \underbrace{\left[\Psi_N \Psi_N^* \right]}_{\text{Nuclear WF}} \underbrace{\langle N | \bar{\psi}(0) u[0, r] \psi(r) | N \rangle}_{\text{Nucleonic TMD}} \underbrace{\left[\langle (A-1) | \mathcal{U}[0, r] | (A-1) \rangle \right]}_{\text{Classical Rescattering}}$$

Quasi-Classical Factorization

$$\begin{aligned}
 \underbrace{\Phi_{\alpha\beta}^A(x, \vec{k}_\perp)}_{\text{Nuclear TMD's}} &= \frac{A}{(2\pi)^5} \sum_{\sigma\sigma'} \int d^2+ p d^2- b d^2 r d^2 k' e^{-i(\vec{k}_\perp - \vec{k}'_\perp - \hat{x} \vec{p}_\perp) \cdot \vec{r}_\perp} \\
 &\times W_{\sigma'\sigma}(p, b) \underbrace{[\phi_{\alpha\beta}^N(\hat{x}, \vec{k}'_\perp)]_{\sigma\sigma'}}_{\text{Nucleonic TMD's}} S_{(r_T, b_T)}^{[\infty^-, b^-]}
 \end{aligned}$$

$\hat{x} \equiv \frac{P^+}{p^+} x$

Quasi-Classical Factorization

$$\begin{aligned}
 \underbrace{\Phi_{\alpha\beta}^A(x, \vec{k}_\perp)}_{\text{Nuclear TMD's}} &= \frac{A}{(2\pi)^5} \sum_{\sigma\sigma'} \int d^2+ p d^2- b d^2 r d^2 k' e^{-i(\vec{k}_\perp - \vec{k}'_\perp - \hat{x} \vec{p}_\perp) \cdot \vec{r}_\perp} \\
 &\times \underbrace{W_{\sigma'\sigma}(p, b)}_{\text{Wigner Distribution (Nuclear WF's)}} \underbrace{[\phi_{\alpha\beta}^N(\hat{x}, \vec{k}'_\perp)]_{\sigma\sigma'}}_{\text{Nucleonic TMD's}} S_{(r_T, b_T)}^{[\infty^-, b^-]}
 \end{aligned}$$

$\hat{x} \equiv \frac{P^+}{p^+} x$

$$W_{\sigma'\sigma}(\bar{p}, b) = \frac{1}{2(2\pi)^3} \int \frac{d^2+(p-p')}{\sqrt{p^+ p'^+}} e^{-i(p-p') \cdot b} \Psi_\sigma^N(p) \Psi_{\sigma'}^{N*}(p')$$

“Average” phase space distribution of nucleons in the nucleus: Leading Order in $A^{1/3}$

Quasi-Classical Factorization

$$\begin{aligned}
 \underbrace{\Phi_{\alpha\beta}^A(x, \vec{k}_\perp)}_{\text{Nuclear TMD's}} &= \frac{A}{(2\pi)^5} \sum_{\sigma\sigma'} \int d^2+ p d^2- b d^2 r d^2 k' e^{-i(\vec{k}_\perp - \vec{k}'_\perp - \hat{x} \vec{p}_\perp) \cdot \vec{r}_\perp} \\
 &\times \underbrace{W_{\sigma'\sigma}(p, b)}_{\text{Wigner Distribution (Nuclear WF's)}} \underbrace{[\phi_{\alpha\beta}^N(\hat{x}, \vec{k}'_\perp)]_{\sigma\sigma'}}_{\text{Nucleonic TMD's}} \underbrace{S_{(r_T, b_T)}^{[\infty^-, b^-]}}_{\text{Gauge Link (Classical)}}
 \end{aligned}$$

$\hat{x} \equiv \frac{P^+}{p^+} x$

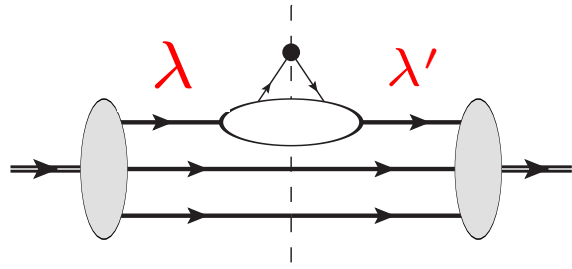
$$W_{\sigma'\sigma}(\vec{p}, b) = \frac{1}{2(2\pi)^3} \int \frac{d^2+ (p-p')}{\sqrt{p^+ p'^+}} e^{-i(p-p') \cdot b} \Psi_\sigma^N(p) \Psi_{\sigma'}^{N*}(p')$$

“Average” phase space distribution of nucleons in the nucleus: Leading Order in $A^{1/3}$

$$S_{(r_T, b_T)}^{[\infty^-, b^-]} = \exp \left[-\frac{1}{4} r_T^2 Q_s^2(b_T) \left(\frac{R^-(b_T) - b^-}{2R^-(b_T)} \right) \right]$$

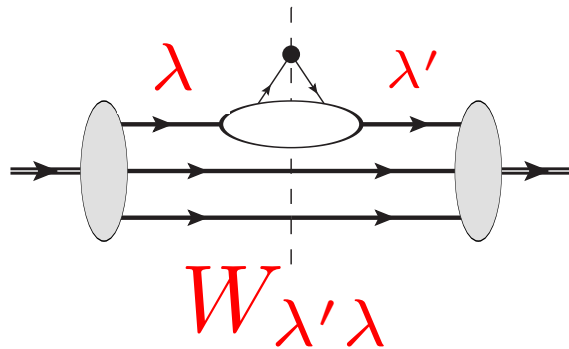
Multiple rescattering on spectator nucleons: Resums $\alpha_s^2 A^{1/3} \sim \mathcal{O}(1)$

Spin Structure of an Unpolarized Nucleus



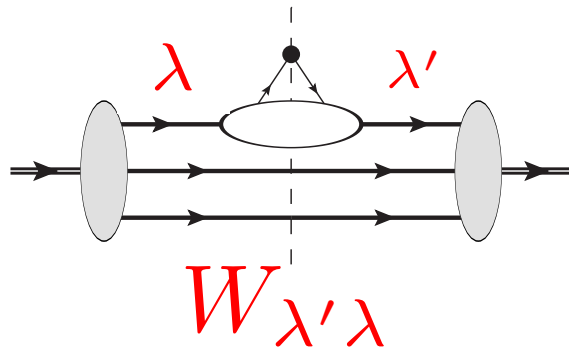
- Consider for simplicity an unpolarized nucleus.

Spin Structure of an Unpolarized Nucleus



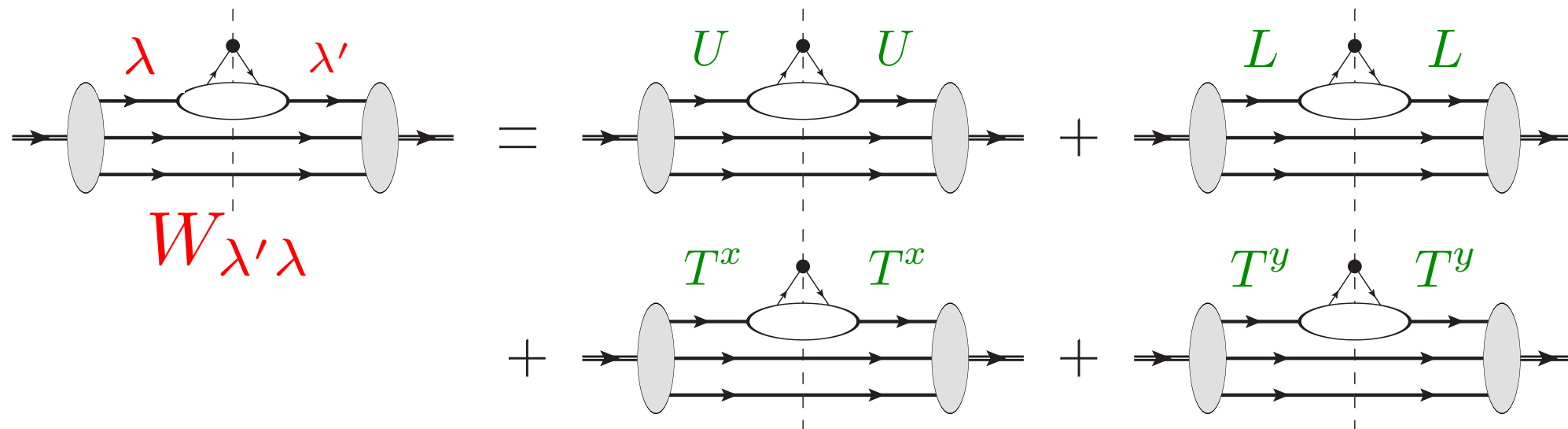
- Consider for simplicity an unpolarized nucleus.
- The spin of the **nucleons** is described by the **2 x 2 density matrix** $W_{\lambda'\lambda}$
 - In the rest frame: $[W]_{\lambda'\lambda} = W_{unp}[1]_{\lambda'\lambda} + \vec{W}_{pol} \cdot [\vec{\sigma}]_{\lambda'\lambda}$
$$W(\vec{p}, \vec{b}, \vec{S}) = W_{unp}(\vec{p}, \vec{b}) + \vec{S} \cdot \vec{W}_{pol}(\vec{p}, \vec{b})$$

Spin Structure of an Unpolarized Nucleus



- Consider for simplicity an unpolarized nucleus.
- The spin of the **nucleons** is described by the **2 x 2 density matrix** $W_{\lambda'\lambda}$
 - In the rest frame: $[W]_{\lambda'\lambda} = W_{unp}[1]_{\lambda'\lambda} + \vec{W}_{pol} \cdot [\vec{\sigma}]_{\lambda'\lambda}$
$$W(\vec{p}, \vec{b}, \vec{S}) = W_{unp}(\vec{p}, \vec{b}) + \vec{S} \cdot \vec{W}_{pol}(\vec{p}, \vec{b})$$
 - Generalize to **covariant spin vector** by boosting from the rest frame.

Spin Structure of an Unpolarized Nucleus



- Consider for simplicity an unpolarized nucleus.
- The spin of the **nucleons** is described by the **2 x 2 density matrix** $W_{\lambda'\lambda}$
 - In the rest frame: $[W]_{\lambda'\lambda} = W_{unp}[1]_{\lambda'\lambda} + \vec{W}_{pol} \cdot [\vec{\sigma}]_{\lambda'\lambda}$
 $W(\vec{p}, \vec{b}, \vec{S}) = W_{unp}(\vec{p}, \vec{b}) + \vec{S} \cdot \vec{W}_{pol}(\vec{p}, \vec{b})$
 - Generalize to **covariant spin vector** by boosting from the rest frame.
- The nucleons can have any of 4 polarizations: **unpolarized, longitudinal, and transverse (x and y)**

Symmetries of the Nuclear Wave Function

$$W_{\sigma'\sigma}(\bar{p}, b) = \frac{1}{2(2\pi)^3} \int \frac{d^2{}^+(p-p')}{\sqrt{p^+ p'^+}} e^{-i(p-p')\cdot b} \Psi_{\sigma}^N(p) \Psi_{\sigma'}^{N*}(p')$$

- Since the Wigner distribution is built only from the nuclear wave functions (no gauge link), it has a **high degree of symmetry**:

Symmetries of the Nuclear Wave Function

$$W_{\sigma'\sigma}(\bar{p}, b) = \frac{1}{2(2\pi)^3} \int \frac{d^2+(p-p')}{\sqrt{p^+ p'^+}} e^{-i(p-p')\cdot b} \Psi_{\sigma}^N(p) \Psi_{\sigma'}^{N*}(p')$$

- Since the Wigner distribution is built only from the nuclear wave functions (no gauge link), it has a **high degree of symmetry**:

- **Discrete symmetries**: P and T

Symmetries of the Nuclear Wave Function

$$W_{\sigma'\sigma}(\bar{p}, b) = \frac{1}{2(2\pi)^3} \int \frac{d^2+(p-p')}{\sqrt{p^+ p'^+}} e^{-i(p-p')\cdot b} \Psi_{\sigma}^N(p) \Psi_{\sigma'}^{N*}(p')$$

- Since the Wigner distribution is built only from the nuclear wave functions (no gauge link), it has a **high degree of symmetry**:

- **Discrete symmetries**: P and T

- Independent of the **collision axis** (direction of gauge link)

Symmetries of the Nuclear Wave Function

$$W_{\sigma'\sigma}(\bar{p}, b) = \frac{1}{2(2\pi)^3} \int \frac{d^2+(p-p')}{\sqrt{p^+p'^+}} e^{-i(p-p')\cdot b} \Psi_{\sigma}^N(p) \Psi_{\sigma'}^{N*}(p')$$

- Since the Wigner distribution is built only from the nuclear wave functions (no gauge link), it has a **high degree of symmetry**:

- **Discrete symmetries**: P and T

- Independent of the **collision axis** (direction of gauge link)

- In the nuclear **rest frame** (assuming **non-relativistic** nucleon motion)

$$W_{\sigma'\sigma}(\vec{p}, \vec{b}) = \frac{1}{2(2\pi)^3 m_N} \int d^3(p - p') e^{+i(\vec{p}-\vec{p}')\cdot\vec{b}} \Psi_{\sigma}^N(\vec{p}^2) \Psi_{\sigma'}^{N*}(\vec{p}'^2)$$

Symmetries of the Nuclear Wave Function

$$W_{\sigma'\sigma}(\bar{p}, b) = \frac{1}{2(2\pi)^3} \int \frac{d^2+(p-p')}{\sqrt{p^+ p'^+}} e^{-i(p-p') \cdot b} \Psi_{\sigma}^N(p) \Psi_{\sigma'}^{N*}(p')$$

- Since the Wigner distribution is built only from the nuclear wave functions (no gauge link), it has a **high degree of symmetry**:

- **Discrete symmetries**: P and T

- Independent of the **collision axis** (direction of gauge link)

- In the nuclear **rest frame** (assuming **non-relativistic** nucleon motion)

$$W_{\sigma'\sigma}(\vec{p}, \vec{b}) = \frac{1}{2(2\pi)^3 m_N} \int d^3(p - p') e^{+i(\vec{p}-\vec{p}') \cdot \vec{b}} \Psi_{\sigma}^N(\vec{p}^2) \Psi_{\sigma'}^{N*}(\vec{p}'^2)$$

- **3D Rotational Symmetry**

Symmetries of the Nuclear Wave Function

$$W_{\sigma'\sigma}(\bar{p}, b) = \frac{1}{2(2\pi)^3} \int \frac{d^2+(p-p')}{\sqrt{p^+ p'^+}} e^{-i(p-p')\cdot b} \Psi_{\sigma}^N(p) \Psi_{\sigma'}^{N*}(p')$$

- Since the Wigner distribution is built only from the nuclear wave functions (no gauge link), it has a **high degree of symmetry**:

- **Discrete symmetries**: P and T

- Independent of the **collision axis** (direction of gauge link)

- In the nuclear **rest frame** (assuming **non-relativistic** nucleon motion)

$$W_{\sigma'\sigma}(\vec{p}, \vec{b}) = \frac{1}{2(2\pi)^3 m_N} \int d^3(p - p') e^{+i(\vec{p}-\vec{p}')\cdot\vec{b}} \Psi_{\sigma}^N(\vec{p}^2) \Psi_{\sigma'}^{N*}(\vec{p}'^2)$$

- **3D Rotational Symmetry**

?

Proton: **Relativistically** moving partons....
...**Lorentz-Invariance Relations??**

D. Pitonyak

Parameterization of the Wigner Distribution

- Imposing **P**, **T**, and **3D rotation** symmetry:

$$W(\vec{p}, \vec{b}, \vec{S}) = W_{unp}[\vec{p}^2, \vec{b}^2, (\vec{p} \cdot \vec{b})^2] \\ + \vec{S} \cdot (\vec{b} \times \vec{p}) W_{OAM}[\vec{p}^2, \vec{b}^2, (\vec{p} \cdot \vec{b})^2]$$

$\vec{L} \cdot \vec{S}$ Spin-Orbit Coupling!

Parameterization of the Wigner Distribution

- Imposing **P**, **T**, and **3D rotation** symmetry:

$$W(\vec{p}, \vec{b}, \vec{S}) = W_{unp}[\vec{p}^2, \vec{b}^2, (\vec{p} \cdot \vec{b})^2] \\ + \underbrace{\vec{S} \cdot (\vec{b} \times \vec{p})}_{\vec{L} \cdot \vec{S} \text{ Spin-Orbit Coupling!}} W_{OAM}[\vec{p}^2, \vec{b}^2, (\vec{p} \cdot \vec{b})^2]$$

- Gets **integrated** over impact parameters with the **gauge link** possessing **2D rotation** symmetry:

$$\int d^2b W(\vec{p}, \vec{b}, \vec{S}) S(b_T)$$

$$b_{\perp}^i b_{\perp}^j \rightarrow \frac{1}{2} b_T^2 \delta^{ij}$$

Parameterization of the Wigner Distribution

- Imposing **P**, **T**, and **3D rotation** symmetry:

$$W(\vec{p}, \vec{b}, \vec{S}) = W_{unp}[\vec{p}^2, \vec{b}^2, (\vec{p} \cdot \vec{b})^2] \\ + \underbrace{\vec{S} \cdot (\vec{b} \times \vec{p})}_{\vec{L} \cdot \vec{S} \text{ Spin-Orbit Coupling!}} W_{OAM}[\vec{p}^2, \vec{b}^2, (\vec{p} \cdot \vec{b})^2]$$

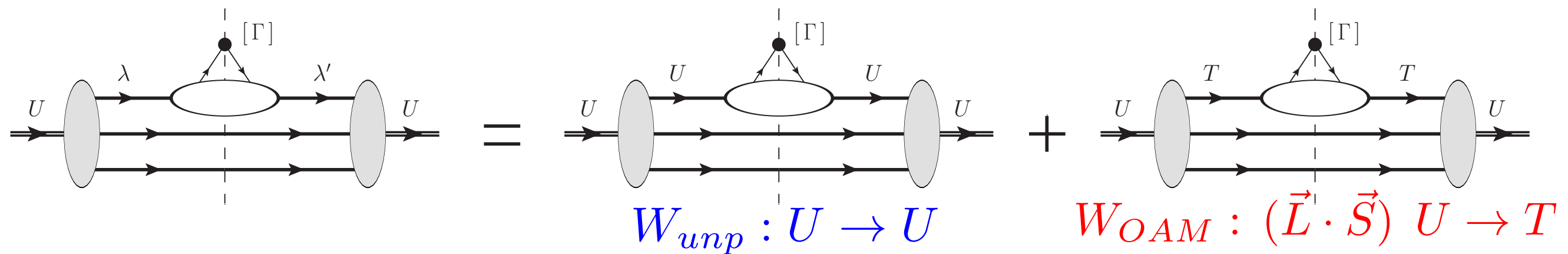
- Gets **integrated** over impact parameters with the **gauge link** possessing **2D rotation** symmetry:

$$\int d^2b W(\vec{p}, \vec{b}, \vec{S}) S(b_T) \quad \boxed{b_{\perp}^i b_{\perp}^j \rightarrow \frac{1}{2} b_T^2 \delta^{ij}}$$

- The **maximum spin-orbit structure** of the unpolarized nucleus is

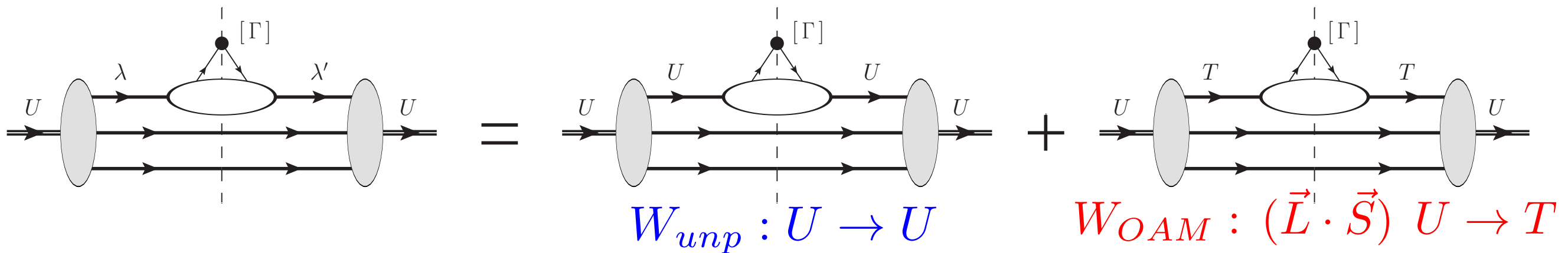
$$W(\vec{p}, \vec{b}, \vec{S}) \Rightarrow W_{unp}[p_T^2, b_T^2; p_z^2, b_z^2] \\ + \underbrace{b_z (\vec{p}_{\perp} \times \vec{S}_{\perp})}_{\text{Depth Dependence!}} W_{OAM}[p_T^2, b_T^2; p_z^2, b_z^2]$$

TMD's of an Unpolarized Nucleus



- For an unpolarized nucleus, two channels survive:
 - **Unpolarized** nucleons: trivial channel
 - **Transversely-polarized** nucleons: **OAM** channel

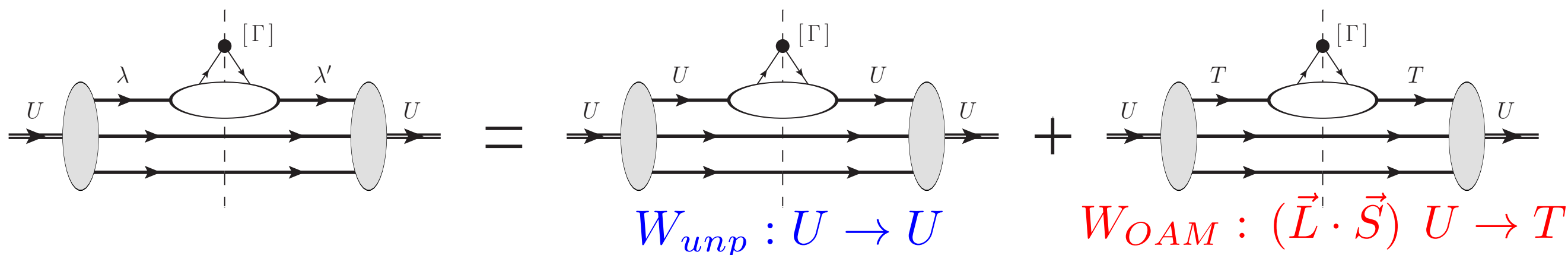
TMD's of an Unpolarized Nucleus



- For an unpolarized nucleus, two channels survive:
 - **Unpolarized** nucleons: trivial channel
 - **Transversely-polarized** nucleons: **OAM** channel
- An unpolarized nucleus has **2 leading-twist TMD's**:

$$\Phi^A(x, \vec{k}_\perp) = f_1^A \left[\frac{1}{2} \gamma^- \right] - \left(\frac{k_\perp^j}{M_A} h_1^{\perp A} \right) \left[\frac{i}{2} \gamma_\perp^j \gamma^- \right]$$

TMD's of an Unpolarized Nucleus

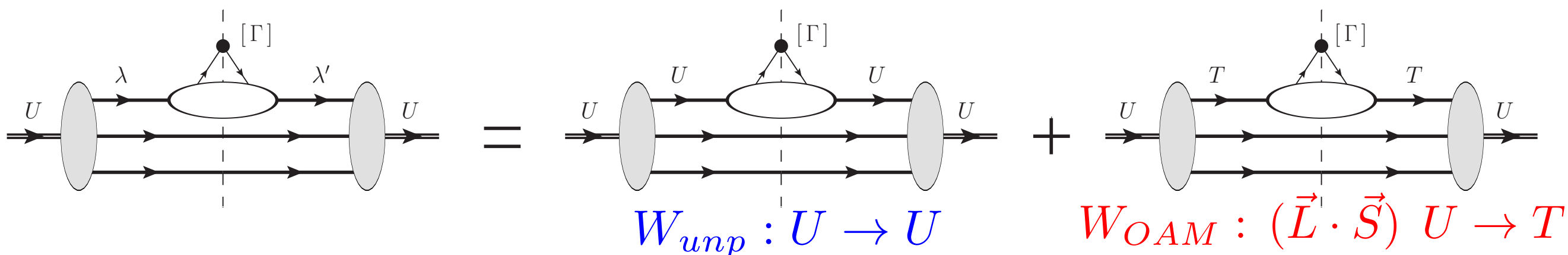


- For an unpolarized nucleus, two channels survive:
 - **Unpolarized** nucleons: trivial channel
 - **Transversely-polarized** nucleons: **OAM** channel
- An unpolarized nucleus has **2 leading-twist TMD's**:

$$\Phi^A(x, \vec{k}_\perp) = \underline{f_1^A} \left[\frac{1}{2} \gamma^- \right] - \left(\frac{k_\perp^j}{M_A} h_1^{\perp A} \right) \left[\frac{i}{2} \gamma_\perp^j \gamma^- \right]$$

Unpolarized quarks, azimuthally symmetric

TMD's of an Unpolarized Nucleus



- For an unpolarized nucleus, two channels survive:
 - **Unpolarized** nucleons: trivial channel
 - **Transversely-polarized** nucleons: **OAM** channel
- An unpolarized nucleus has **2 leading-twist TMD's**:

$$\Phi^A(x, \vec{k}_\perp) = \underbrace{f_1^A \left[\frac{1}{2} \gamma^- \right]}_{\text{Unpolarized quarks, azimuthally symmetric}} - \left(\frac{k_\perp^j}{M_A} h_1^{\perp A} \right) \left[\frac{i}{2} \gamma_\perp^j \gamma^- \right]$$

Unpolarized quarks, azimuthally symmetric

Boer-Mulders Distribution: Transversely polarized quarks, azimuthally antisymmetric

Unpolarized Quark Distribution f_1^A

$$f_1^A = \text{Diagram 1} + \text{Diagram 2}$$

Diagram 1: A horizontal line with three parallel arrows pointing right. The top arrow is labeled U . The line is flanked by two gray vertical ellipses. Above the line, a vertex labeled U is connected to the top arrow by two lines forming a triangle. Below the line, a vertical line connects to a circle with a cross inside, labeled $W_{unp} \otimes f_1^N$.

Diagram 2: A horizontal line with three parallel arrows pointing right. The top arrow is labeled T . The line is flanked by two gray vertical ellipses. Above the line, a vertex labeled U is connected to the top arrow by two lines forming a triangle. Below the line, a vertical line connects to a circle with a cross inside, labeled $W_{OAM} \otimes f_{1T}^{\perp N}$.

$$f_1^A(x, k_T) = \frac{2A}{(2\pi)^5} \int d^2+ p d^2- b d^2 r d^2 k' e^{-i(\vec{k}_\perp - \vec{k}'_\perp - \hat{x} \vec{p}_\perp)} S_{(r_T, b_T)}^{[\infty^-, b^-]}$$

$$\times \left(W_{unp}(p, b) f_1^N(\hat{x}, k'_T) - \frac{P^+ b^-}{A m_N^2} (\vec{p}_\perp \cdot \vec{k}'_\perp) W_{OAM}(p, b) f_{1T}^{\perp N}(\hat{x}, k'_T) \right)$$

Unpolarized Quark Distribution f_1^A

$$f_1^A = \underbrace{\text{Diagram 1}}_{W_{unp} \otimes f_1^N} + \text{Diagram 2}$$

Diagram 1: A horizontal line with three parallel arrows pointing right. The top arrow is labeled 'U'. It passes through two gray vertical ellipses. Above the line, a vertex labeled 'U' has two arrows pointing down to the top and bottom lines. Below the line, a vertical dashed line connects to a circle with a cross inside. Below this circle is the label $W_{unp} \otimes f_1^N$.

Diagram 2: A horizontal line with three parallel arrows pointing right. The top arrow is labeled 'T'. It passes through two gray vertical ellipses. Above the line, a vertex labeled 'U' has two arrows pointing down to the top and bottom lines. Below the line, a vertical dashed line connects to a circle with a cross inside. Below this circle is the label $W_{OAM} \otimes f_{1T}^{\perp N}$.

$$f_1^A(x, k_T) = \frac{2A}{(2\pi)^5} \int d^2+ p d^2- b d^2 r d^2 k' e^{-i(\vec{k}_\perp - \vec{k}'_\perp - \hat{x} \vec{p}_\perp)} S_{(r_T, b_T)}^{[\infty^-, b^-]}$$

$$\times \left(\underbrace{W_{unp}(p, b) f_1^N(\hat{x}, k'_T)} - \frac{P^+ b^-}{A m_N^2} (\vec{p}_\perp \cdot \vec{k}'_\perp) W_{OAM}(p, b) f_{1T}^{\perp N}(\hat{x}, k'_T) \right)$$

Unpolarized Channel: $f_1^N \rightarrow f_1^A$

- Trivial density distribution + momentum broadening

Unpolarized Quark Distribution f_1^A

$$f_1^A = \underbrace{\text{Diagram 1}}_{W_{unp} \otimes f_1^N} + \underbrace{\text{Diagram 2}}_{W_{OAM} \otimes f_{1T}^{\perp N}}$$

$$f_1^A(x, k_T) = \frac{2A}{(2\pi)^5} \int d^2+ p d^2- b d^2 r d^2 k' e^{-i(\vec{k}_\perp - \vec{k}'_\perp - \hat{x} \vec{p}_\perp)} S_{(r_T, b_T)}^{[\infty^-, b^-]} \times \left(\underbrace{W_{unp}(p, b) f_1^N(\hat{x}, k'_T)}_{\text{blue}} - \underbrace{\frac{P^+ b^-}{A m_N^2} (\vec{p}_\perp \cdot \vec{k}'_\perp) W_{OAM}(p, b) f_{1T}^{\perp N}(\hat{x}, k'_T)}_{\text{red}} \right)$$

Unpolarized Channel: $f_1^N \rightarrow f_1^A$

- **Trivial density distribution** + momentum broadening

OAM Channel: $f_{1T}^{\perp N} \rightarrow f_1^A$

- **“Dipole modulation”**: Sivers function + momentum broadening

Boer-Mulders Distribution $h_1^{\perp A}$

$$h_1^{\perp A} = \text{Diagram 1} + \text{Diagram 2}$$

Diagram 1: A horizontal line with three parallel arrows pointing right. The top arrow is labeled U , the middle arrow is labeled U , and the bottom arrow is labeled U . Above the middle arrow is a vertex labeled T with two arrows pointing down to the top and bottom arrows. Below the middle arrow is a vertex labeled $W_{unp} \otimes h_1^{\perp N}$ with a vertical line connecting it to the middle arrow. The diagram is flanked by two gray ovals.

Diagram 2: A horizontal line with three parallel arrows pointing right. The top arrow is labeled T , the middle arrow is labeled T , and the bottom arrow is labeled U . Above the middle arrow is a vertex labeled T with two arrows pointing down to the top and bottom arrows. Below the middle arrow is a vertex labeled $W_{OAM} \otimes (h_1^N + h_{1T}^{\perp N})$ with a vertical line connecting it to the middle arrow. The diagram is flanked by two gray ovals.

$$h_1^{\perp A}(x, k_T) = \frac{2A}{(2\pi)^5} \frac{Am_N}{k_T^2} \int d^2+ p d^2- b d^2 r d^2 k' e^{-i(\vec{k}_{\perp} - \vec{k}'_{\perp} - \hat{x} \vec{p}_{\perp}) \cdot \vec{r}_{\perp}} S_{(r_T, b_T)}^{[\infty^-, b^-]}$$

$$\times \left(\frac{\vec{k}_{\perp} \cdot \vec{k}'_{\perp}}{m_N} W_{unp}(p, b) h_1^{\perp N}(\hat{x}, k'_T) - \frac{P^+ b^-}{Am_N} (\vec{p}_{\perp} \cdot \vec{k}_{\perp}) W_{OAM}(p, b) h_1^N(\hat{x}, k'_T) \right.$$

$$\left. - \frac{P^+ b^-}{Am_N} \left(\frac{(\vec{p}_{\perp} \times \vec{k}'_{\perp})(\vec{k}_{\perp} \times \vec{k}'_{\perp})}{m_N^2} - \frac{k_T'^2 (\vec{p}_{\perp} \cdot \vec{k}_{\perp})}{2m_N^2} \right) W_{OAM}(p, b) h_{1T}^{\perp N}(\hat{x}, k'_T) \right)$$

Boer-Mulders Distribution $h_1^{\perp A}$

$$h_1^{\perp A} = \underbrace{\text{Diagram 1}}_{W_{unp} \otimes h_1^{\perp N}} + \underbrace{\text{Diagram 2}}_{W_{OAM} \otimes (h_1^N + h_{1T}^{\perp N})}$$

The diagrams represent the decomposition of the Boer-Mulders distribution into unpolarized and orbital angular momentum (OAM) components. Diagram 1 shows a nucleon (grey oval) with a quark (black dot) and a gluon (triangle) interacting via a tensor T and a vector U . Diagram 2 shows a similar interaction but with a different tensor T and vector U .

$$h_1^{\perp A}(x, k_T) = \frac{2A}{(2\pi)^5} \frac{Am_N}{k_T^2} \int d^2+ p d^2- b d^2 r d^2 k' e^{-i(\vec{k}_{\perp} - \vec{k}'_{\perp} - \hat{x} \vec{p}_{\perp}) \cdot \vec{r}_{\perp}} S_{(r_T, b_T)}^{[\infty^-, b^-]}$$

$$\times \left(\underbrace{\frac{\vec{k}_{\perp} \cdot \vec{k}'_{\perp}}{m_N} W_{unp}(p, b) h_1^{\perp N}(\hat{x}, k'_T)}_{\text{Unpolarized Channel}} - \frac{P^+ b^-}{Am_N} (\vec{p}_{\perp} \cdot \vec{k}_{\perp}) W_{OAM}(p, b) h_1^N(\hat{x}, k'_T) \right.$$

$$\left. - \frac{P^+ b^-}{Am_N} \left(\frac{(\vec{p}_{\perp} \times \vec{k}'_{\perp})(\vec{k}_{\perp} \times \vec{k}'_{\perp})}{m_N^2} - \frac{k_T'^2 (\vec{p}_{\perp} \cdot \vec{k}_{\perp})}{2m_N^2} \right) W_{OAM}(p, b) h_{1T}^{\perp N}(\hat{x}, k'_T) \right)$$

Unpolarized Channel: $h_1^{\perp N} \rightarrow h_1^{\perp A}$

- Trivial density distribution + momentum broadening

Boer-Mulders Distribution $h_1^{\perp A}$

$$h_1^{\perp A} = \underbrace{\text{Diagram 1}}_{W_{unp} \otimes h_1^{\perp N}} + \underbrace{\text{Diagram 2}}_{W_{OAM} \otimes (h_1^N + h_{1T}^{\perp N})}$$

The diagrams show two types of parton distribution functions. Diagram 1 (Unpolarized Channel) shows a parton with momentum U entering a nucleus, interacting with a target T via a dipole interaction, and then exiting. Diagram 2 (OAM Channel) shows a parton with momentum U entering a nucleus, interacting with a target T via a dipole interaction, and then exiting with momentum T . The target T is represented by a triangle with a dot, and the interaction is shown as a dipole (two arrows pointing in opposite directions).

$$h_1^{\perp A}(x, k_T) = \frac{2A}{(2\pi)^5} \frac{Am_N}{k_T^2} \int d^2+ p d^2- b d^2 r d^2 k' e^{-i(\vec{k}_{\perp} - \vec{k}'_{\perp} - \hat{x} \vec{p}_{\perp}) \cdot \vec{r}_{\perp}} S_{(r_T, b_T)}^{[\infty-, b^-]}$$

$$\times \left(\underbrace{\frac{\vec{k}_{\perp} \cdot \vec{k}'_{\perp}}{m_N} W_{unp}(p, b) h_1^{\perp N}(\hat{x}, k'_T)}_{\text{Unpolarized Channel}} - \underbrace{\frac{P^+ b^-}{Am_N} (\vec{p}_{\perp} \cdot \vec{k}_{\perp}) W_{OAM}(p, b) h_1^N(\hat{x}, k'_T)}_{\text{OAM Channel}} \right.$$

$$\left. - \frac{P^+ b^-}{Am_N} \left(\frac{(\vec{p}_{\perp} \times \vec{k}'_{\perp})(\vec{k}_{\perp} \times \vec{k}'_{\perp})}{m_N^2} - \frac{k_T'^2 (\vec{p}_{\perp} \cdot \vec{k}_{\perp})}{2m_N^2} \right) W_{OAM}(p, b) h_{1T}^{\perp N}(\hat{x}, k'_T) \right)$$

Unpolarized Channel: $h_1^{\perp N} \rightarrow h_1^{\perp A}$

- **Trivial density distribution** + momentum broadening

OAM Channel: $h_1^N, h_{1T}^{\perp N} \rightarrow h_1^{\perp A}$

- **“Dipole modulation”**: Transversity + broadening

Boer-Mulders Distribution $h_1^{\perp A}$

$$h_1^{\perp A} = \underbrace{\text{Diagram 1}}_{W_{unp} \otimes h_1^{\perp N}} + \underbrace{\text{Diagram 2}}_{W_{OAM} \otimes (h_1^N + h_{1T}^{\perp N})}$$

The diagrams show two types of parton distribution functions. Diagram 1 (left) represents the unpolarized channel, showing a parton with momentum U entering a target, interacting with a target with momentum T , and exiting with momentum U . Diagram 2 (right) represents the OAM channel, showing a parton with momentum U entering a target, interacting with a target with momentum T , and exiting with momentum U . The interaction is represented by a triangle with a dot at the top vertex.

$$h_1^{\perp A}(x, k_T) = \frac{2A}{(2\pi)^5} \frac{Am_N}{k_T^2} \int d^2+ p d^2- b d^2 r d^2 k' e^{-i(\vec{k}_{\perp} - \vec{k}'_{\perp} - \hat{x} \vec{p}_{\perp}) \cdot \vec{r}_{\perp}} S_{(r_T, b_T)}^{[\infty-, b-]}$$

$$\times \left(\underbrace{\frac{\vec{k}_{\perp} \cdot \vec{k}'_{\perp}}{m_N} W_{unp}(p, b) h_1^{\perp N}(\hat{x}, k'_T)}_{\text{Unpolarized Channel}} - \underbrace{\frac{P^+ b^-}{Am_N} (\vec{p}_{\perp} \cdot \vec{k}_{\perp}) W_{OAM}(p, b) h_1^N(\hat{x}, k'_T)}_{\text{OAM Channel}} \right.$$

$$\left. - \underbrace{\frac{P^+ b^-}{Am_N} \left(\frac{(\vec{p}_{\perp} \times \vec{k}'_{\perp})(\vec{k}_{\perp} \times \vec{k}'_{\perp})}{m_N^2} - \frac{k_T'^2 (\vec{p}_{\perp} \cdot \vec{k}_{\perp})}{2m_N^2} \right) W_{OAM}(p, b) h_{1T}^{\perp N}(\hat{x}, k'_T)}_{\text{OAM Channel}} \right)$$

Unpolarized Channel: $h_1^{\perp N} \rightarrow h_1^{\perp A}$

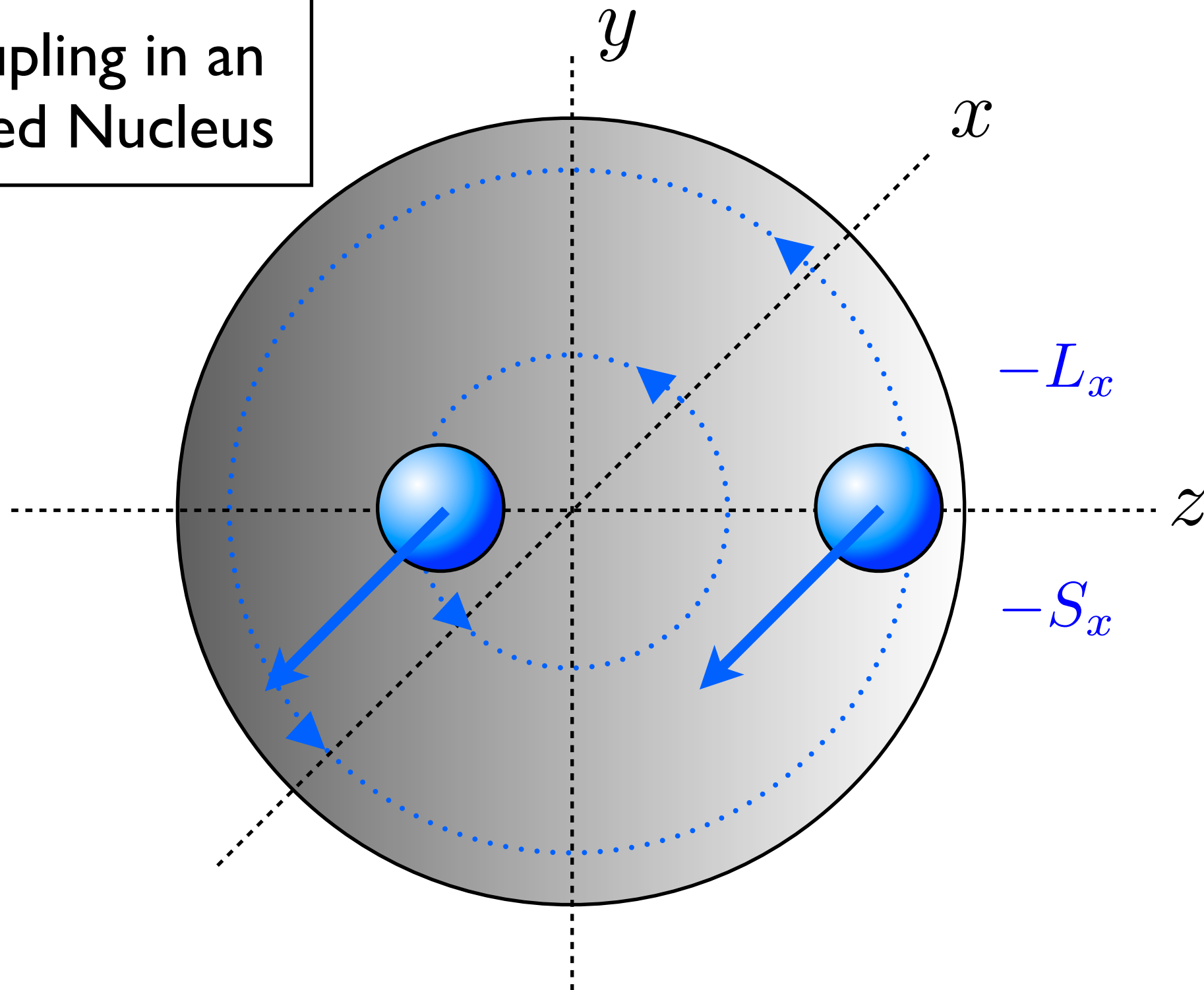
- **Trivial density distribution** + momentum broadening

OAM Channel: $h_1^N, h_{1T}^{\perp N} \rightarrow h_1^{\perp A}$

- **“Dipole modulation”**: Transversity + broadening
- **“Quadrupole modulation”**: Pretzelosity + broadening

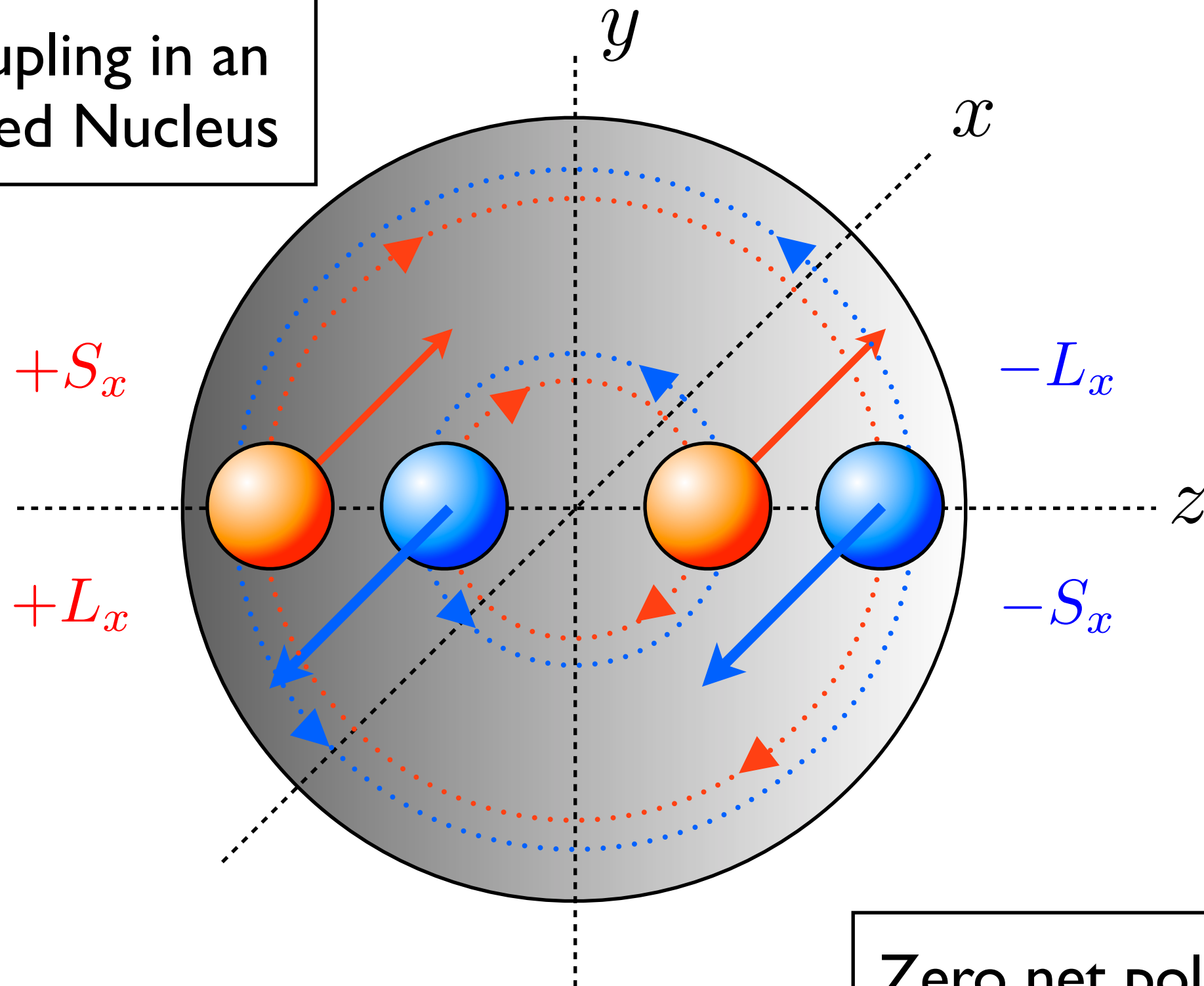
A Physical Illustration: $W_{OAM} + h_1^N \rightarrow h_1^{\perp A}$

$\vec{L} \cdot \vec{S}$ Coupling in an
Unpolarized Nucleus



A Physical Illustration: $W_{OAM} + h_1^N \rightarrow h_1^{\perp A}$

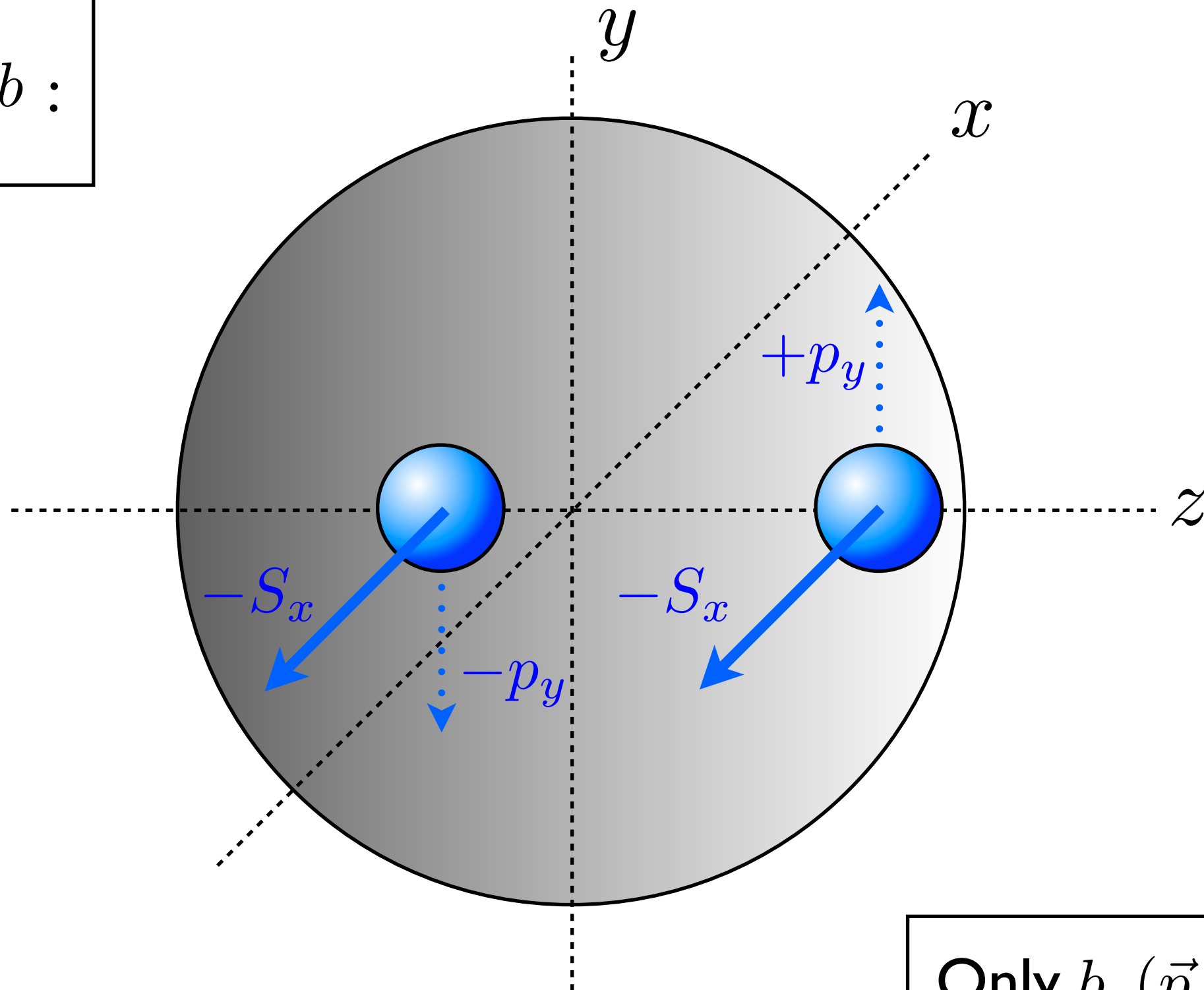
$\vec{L} \cdot \vec{S}$ Coupling in an Unpolarized Nucleus



Zero net polarization.

A Physical Illustration: $W_{OAM} + h_1^N \rightarrow h_1^{\perp A}$

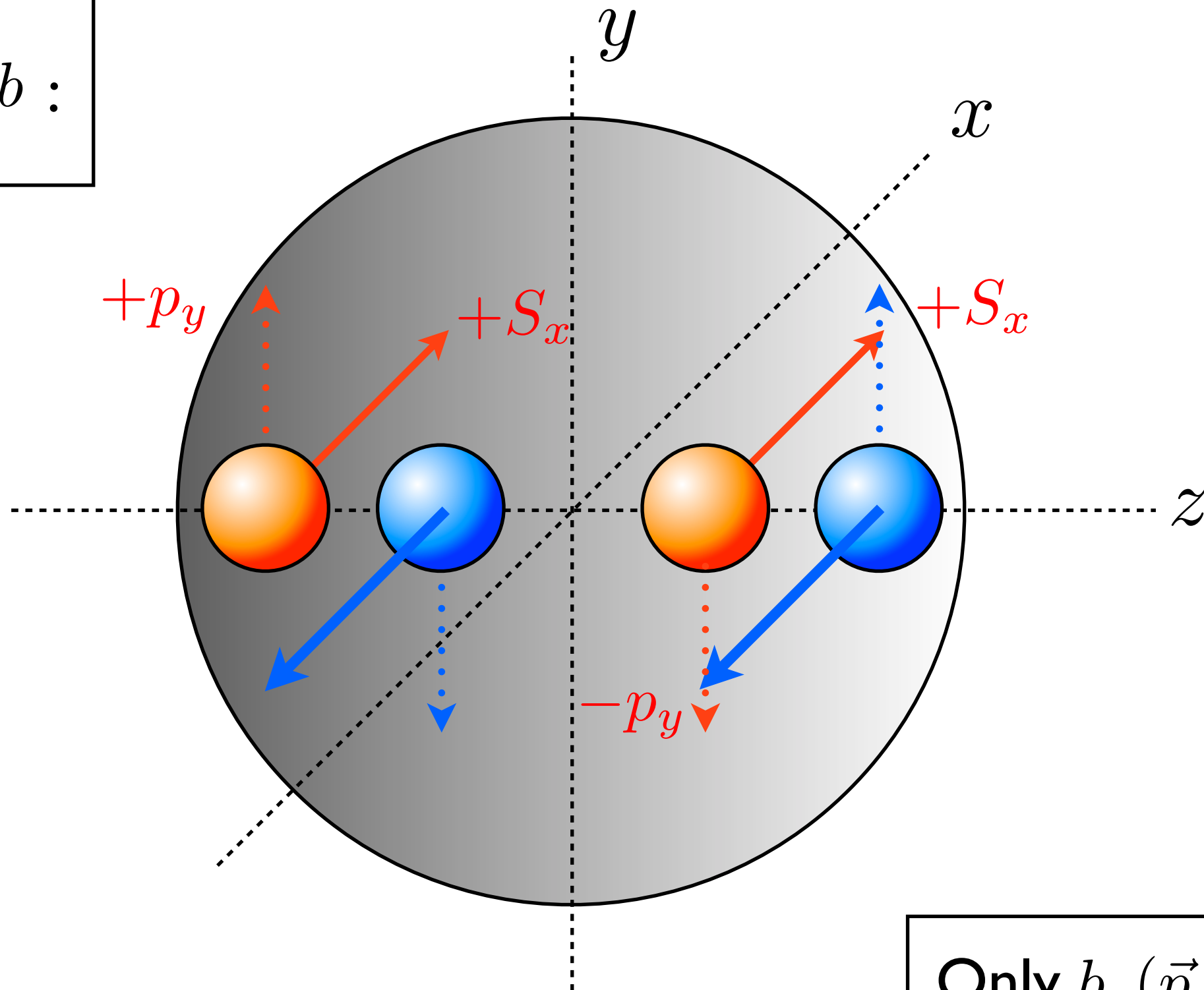
After $\int d^2b :$



Only $b_z(\vec{p}_{\perp} \times \vec{S}_{\perp})$

A Physical Illustration: $W_{OAM} + h_1^N \rightarrow h_1^{\perp A}$

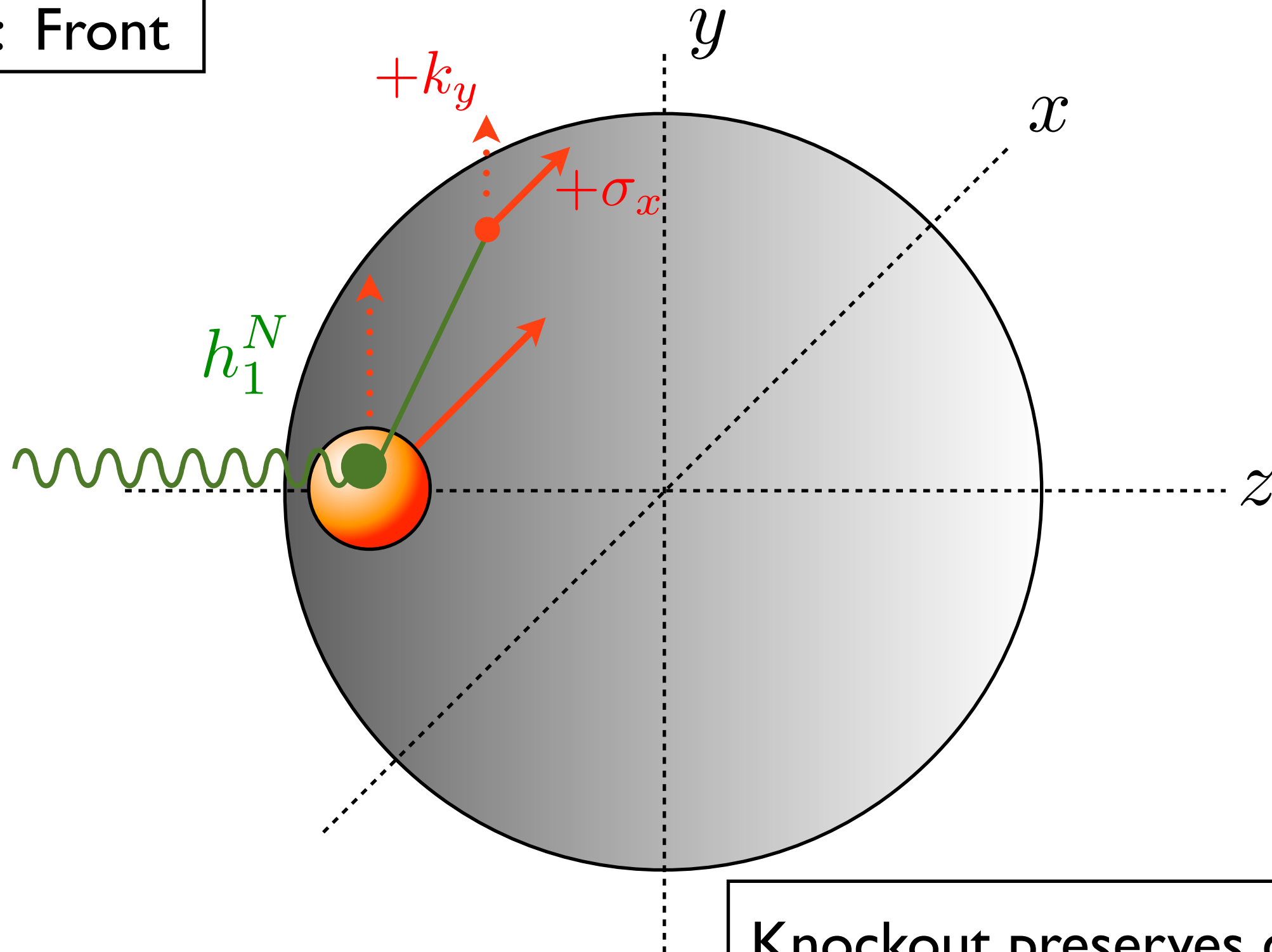
After $\int d^2b :$



Only $b_z(\vec{p}_{\perp} \times \vec{S}_{\perp})$

A Physical Illustration: $W_{OAM} + h_1^N \rightarrow h_1^{\perp A}$

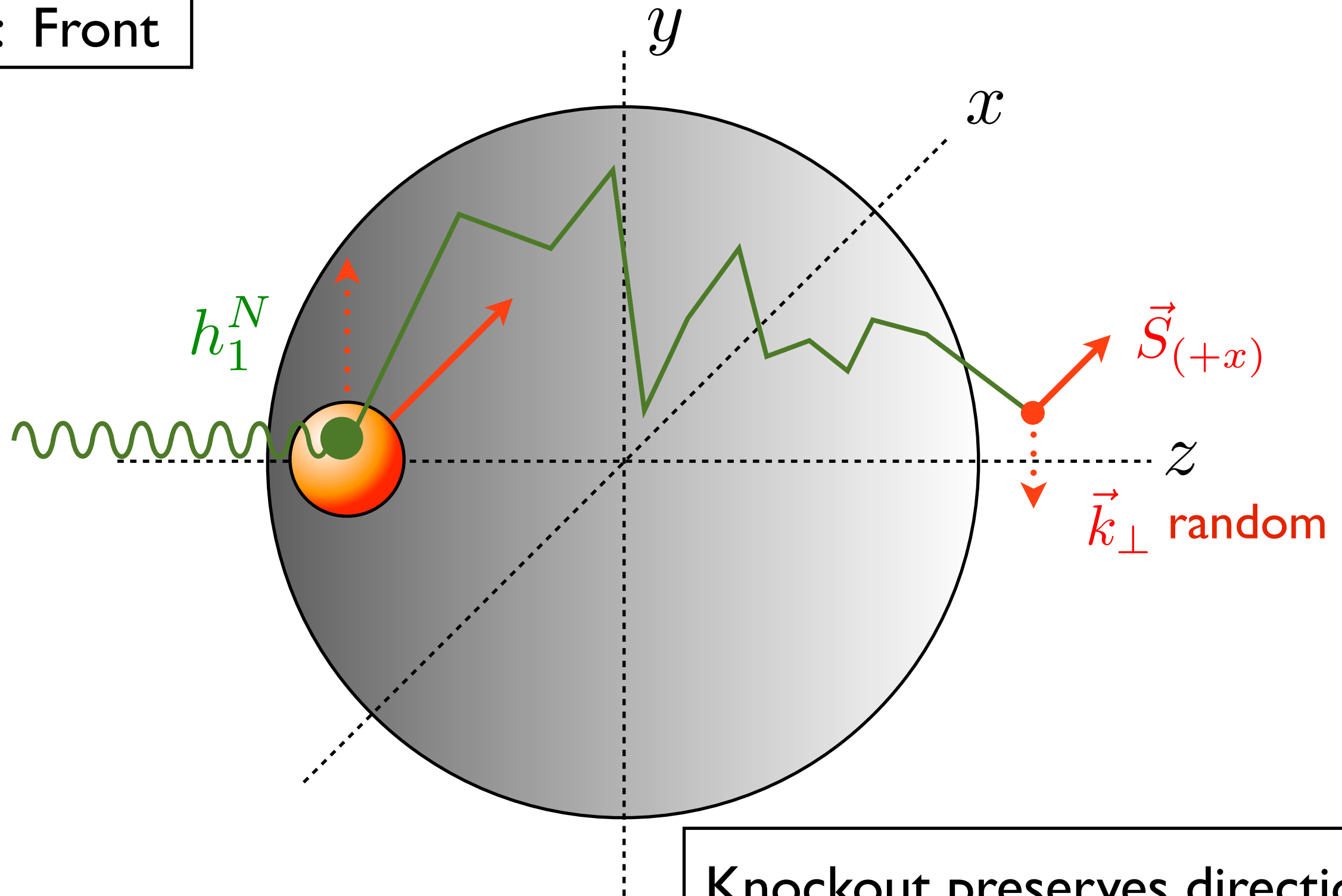
SIDIS: Front



Knockout preserves direction.

A Physical Illustration: $W_{OAM} + h_1^N \rightarrow h_1^{\perp A}$

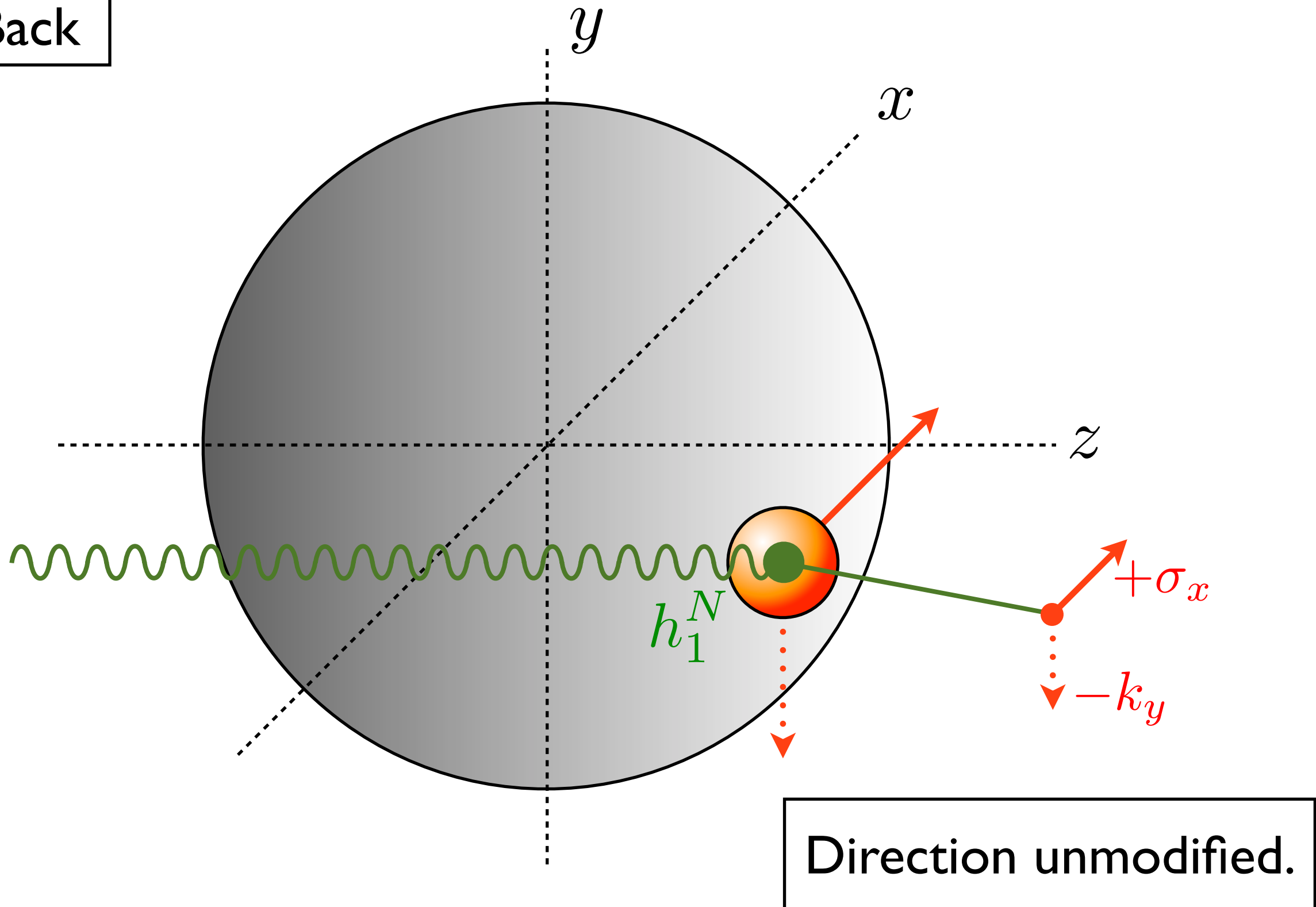
SIDIS: Front



Knockout preserves direction.
But recattering randomizes it.

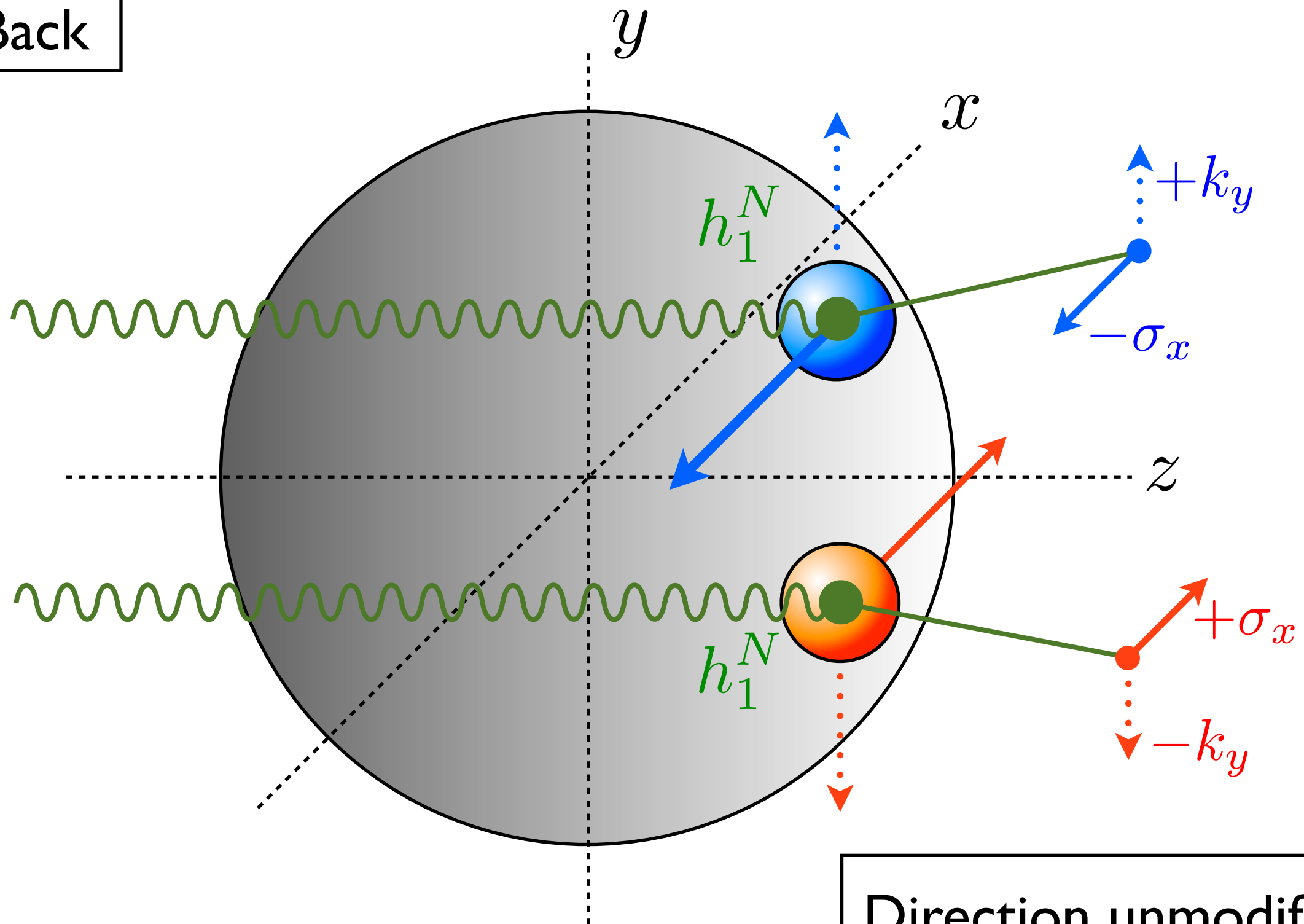
A Physical Illustration: $W_{OAM} + h_1^N \rightarrow h_1^{\perp A}$

SIDIS: Back

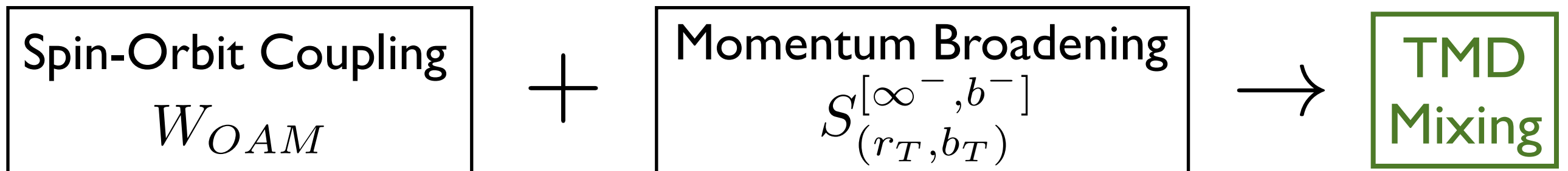


A Physical Illustration: $W_{OAM} + h_1^N \rightarrow h_1^{\perp A}$

SIDIS: Back



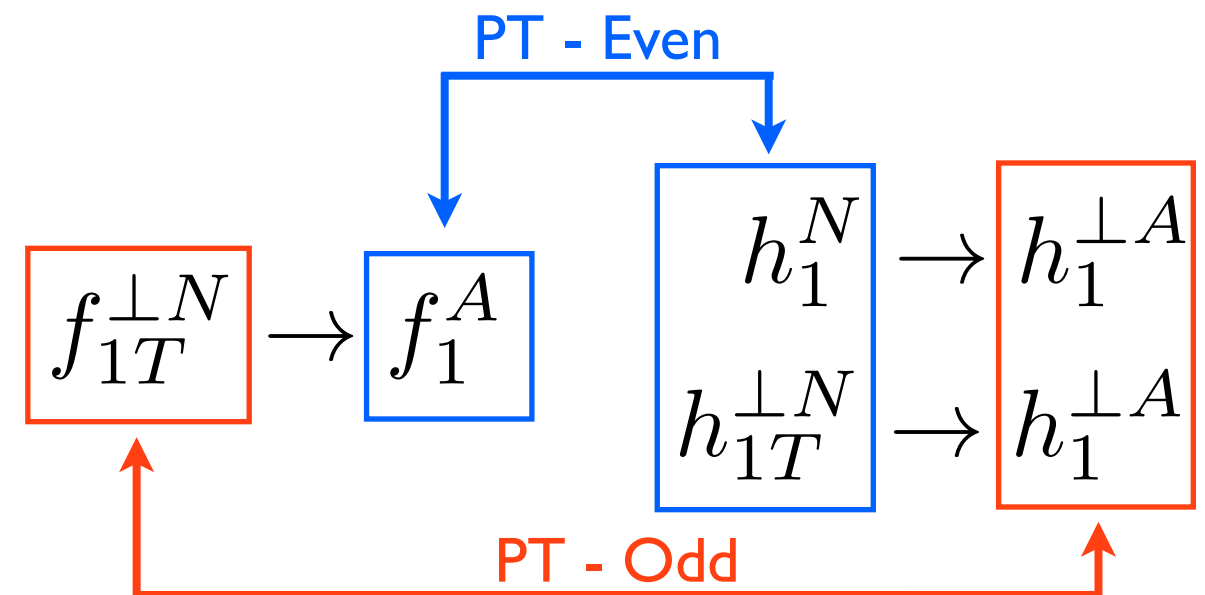
TMD Mixing



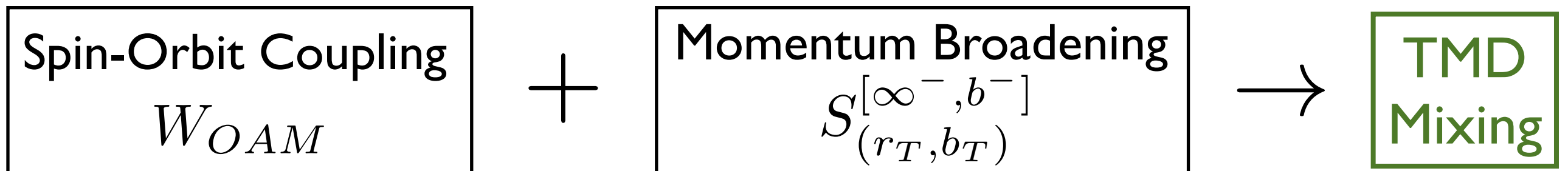
TMD Mixing



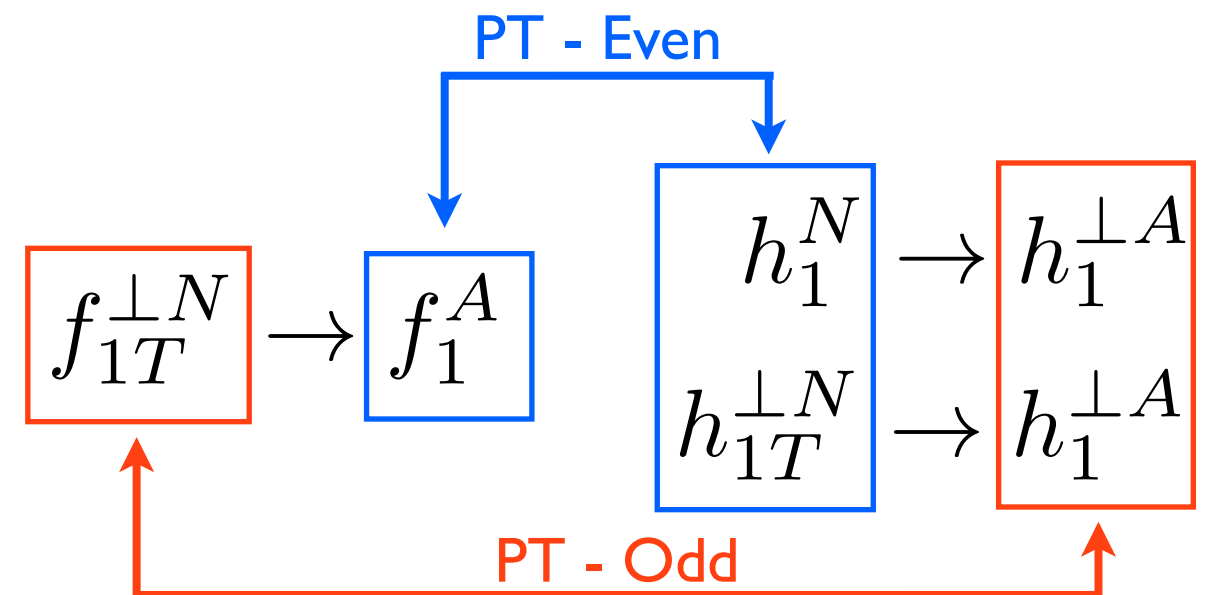
Mixing occurs between the **PT-even** and **PT-odd** sectors:



TMD Mixing



Mixing occurs between the **PT-even** and **PT-odd** sectors:



Multiple rescattering is essential to break **front / back symmetry**

- b_z dependence provides a **PT-reversing** factor
- OAM is not enough: mixing **vanishes** without rescattering.

Implications for an EIC

(1.)

Deviation from
simple broadening?

$$f_1^A \Leftrightarrow f_1^N$$

Presence
of OAM!

Implications for an EIC

(1.)

Deviation from
simple broadening?

$$f_1^A \Leftrightarrow f_1^N$$

Presence
of **OAM**!

(2.)

If the **nucleonic**
TMD's are known...

$$f_1^N \quad f_{1T}^{\perp N}$$

...and the **nuclear**
TMD's are measured...

$$f_1^A \sim f_1^N \otimes W_{unp} + f_1^A \otimes W_{OAM}$$

...can directly
extract OAM

$$W_{OAM} \leftrightarrow \vec{L} \cdot \vec{S}$$

Implications for an EIC

(1.)

Deviation from
simple broadening?

$$f_1^A \Leftrightarrow f_1^N$$

Presence
of **OAM**!

(2.)

If the **nucleonic**
TMD's are known...

...and the **nuclear**
TMD's are measured...

...can directly
extract OAM

$$f_1^N \quad f_{1T}^{\perp N}$$

$$f_1^A \sim f_1^N \otimes W_{unp} + f_1^A \otimes W_{OAM}$$

$$W_{OAM} \leftrightarrow \vec{L} \cdot \vec{S}$$

(3.)

This provides a **prediction** for additional **mixing in other sectors**!

$$h_1^{\perp A} \sim h_1^{\perp N} \otimes W_{unp} + (h_1^N + h_{1T}^{\perp N}) \otimes W_{OAM}$$

Outlook

- TMD mixing is a generic consequence of both spin-orbit coupling and high-density rescattering.

Outlook

- TMD mixing is a generic consequence of both spin-orbit coupling and high-density rescattering.
- Formalism is well-suited to modeling:
 - Choose a form for $W(\vec{p}, \vec{b}, \vec{S}) \longrightarrow$ determines mixing fractions.
 - Use data or simple models for the nucleonic TMD's.
 - Determines the functional form of the nuclear TMD's.

Outlook

- TMD mixing is a generic consequence of both spin-orbit coupling and high-density rescattering.
- Formalism is well-suited to modeling:
 - Choose a form for $W(\vec{p}, \vec{b}, \vec{S}) \longrightarrow$ determines mixing fractions.
 - Use data or simple models for the nucleonic TMD's.
 - Determines the functional form of the nuclear TMD's.
- Ingredients for a systematic global fit:
 - Extensive measurements of the nucleonic TMD's.

Outlook

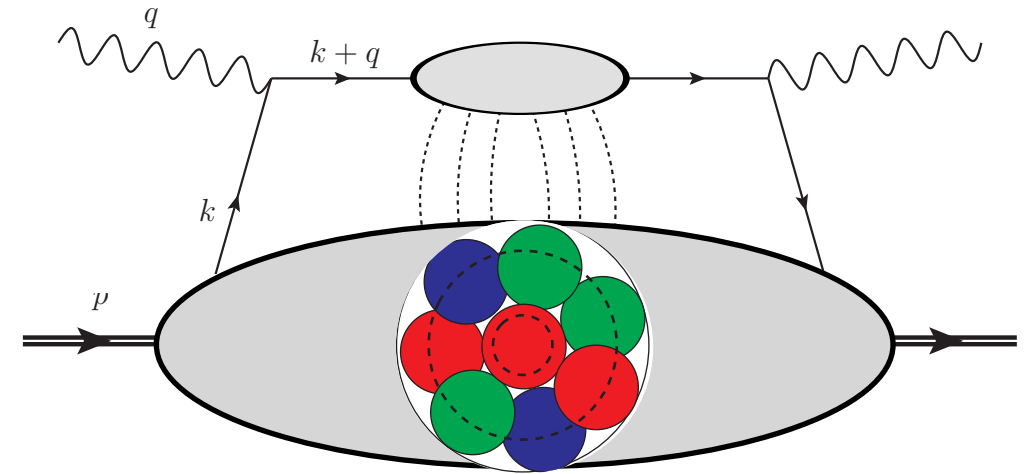
- TMD mixing is a generic consequence of both spin-orbit coupling and high-density rescattering.
- Formalism is well-suited to modeling:
 - Choose a form for $W(\vec{p}, \vec{b}, \vec{S}) \longrightarrow$ determines mixing fractions.
 - Use data or simple models for the nucleonic TMD's.
 - Determines the functional form of the nuclear TMD's.
- Ingredients for a systematic global fit:
 - Extensive measurements of the nucleonic TMD's.
 - Quantum evolution corrections
 - Large- x Q^2 evolution (CSS)
 - Small- x evolution: polarized and unpolarized.

Part II

4:24 pm, “Collective Behavior of Partons”

Summary

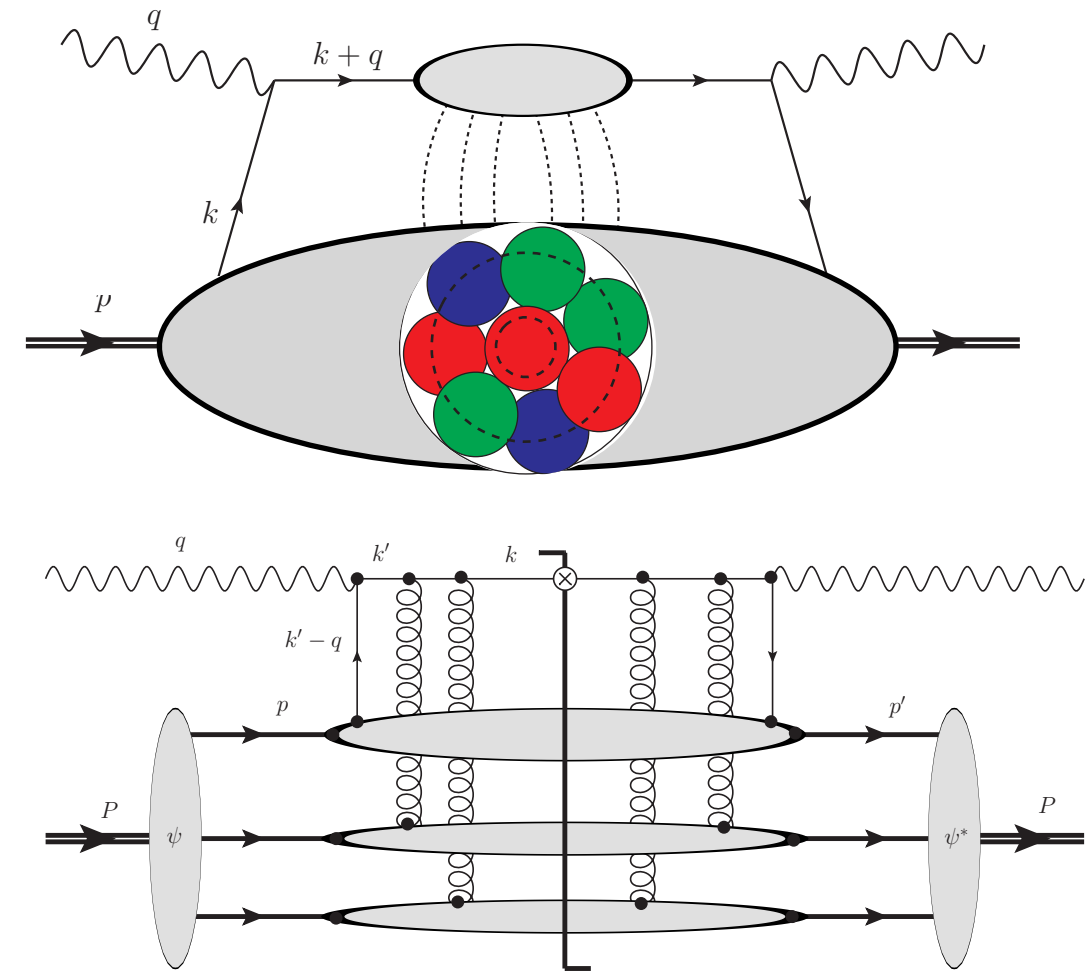
The **gauge link** which is essential for TMD structure represents very different physics at **high density**.



Summary

The **gauge link** which is essential for TMD structure represents very different physics at **high density**.

High-density effects can be **re-summed**, leading to a **quasi-classical factorization** of nuclear TMD's.



Summary

The **gauge link** which is essential for TMD structure represents very different physics at **high density**.

High-density effects can be re-summed, leading to a quasi-classical factorization of nuclear TMD's.

Spin-orbit coupling, together with multiple rescattering, leads to rich TMD mixing with predictive power.

